LLMs Judging LLMs: A Simplex Perspective

Patrick Vossler[1*] **Fan Xia**[1*] **Yifan Mai**[2]

Adarsh Subbaswamy[3] **Jean Feng**[1]

[1]University of California, San Francisco [2]Stanford University

[3]University of Maryland, Baltimore

Abstract

Given the challenge of automatically evaluating free-form outputs from large language models (LLMs), a common solution is to use LLMs themselves as judges, without any gold-standard scores. Implicitly, this practice accounts for only sampling variability (*aleatoric uncertainty*) and ignores uncertainty about judge quality (*epistemic uncertainty*). While this is justified if judges are perfectly accurate, it is unclear when such an approach is theoretically valid and practically robust. We study these questions for the task of ranking LLM candidates from a novel geometric perspective: for M-level scoring systems, both LLM judges and candidates can be represented as points on an $(M-1)$-dimensional probability simplex, where geometric concepts (e.g., triangle areas) correspond to key ranking concepts. This perspective yields intuitive theoretical conditions and visual proofs for when rankings are identifiable; for instance, we provide a formal basis for the "folk wisdom" that LLM judges are more effective for two-level scoring ($M = 2$) than multi-level scoring ($M > 2$). Using this geometric intuition, we design Bayesian priors that encode epistemic uncertainty and vary the priors to conduct sensitivity analyses. Experiments on LLM benchmarks show that rankings based solely on LLM judges are robust in many but not all datasets, underscoring both their widespread success and the need for caution. Our Bayesian method achieves substantially higher coverage rates than existing procedures by modeling epistemic uncertainty.

1 INTRODUCTION

Scalable benchmarking of large language models (LLMs) is increasingly critical given the rapid proliferation of models, model updates, and new benchmark datasets. While multiple choice or numerical answers can be verified algorithmically, many benchmark tasks allow free-form text responses that are more difficult to verify, such as clinical reasoning expressed as natural language or mathematical proofs involving multi-part LaTeX formulas. While the current gold standard of consensus voting by multiple human experts is effective, it is often prohibitively expensive and difficult to scale.

In response to these challenges, recent work has proposed using LLMs themselves as judges (Figure 1) (Zheng et al., 2023b). Here we refer to evaluator LLMs as "judges" and evaluated LLMs as "candidates." This now-common practice effectively treats LLM judges as perfectly accurate, ignoring any uncertainty about their quality and acknowledging only sampling variability (e.g., through bootstrapping or confidence intervals). Borrowing terms from epistemology, the first source of uncertainty is systematic or *epistemic*; due to the lack of gold-standard data, one is uncertain about and cannot determine the true quality of the judges. The second source of uncertainty is stochastic or *aleatoric*; due to sampling variability, there is noise in the returned judge scores but this type of uncertainty can be reduced by increasing sample size. *The goal of this work is to understand how epistemic uncertainty impacts our ability to rank LLM candidates.* We do so by answer-

[*]Equal contribution

Proceedings of the 29[th] International Conference on Artificial Intelligence and Statistics (AISTATS) 2026, Tangier, Morocco. PMLR: Volume 300.

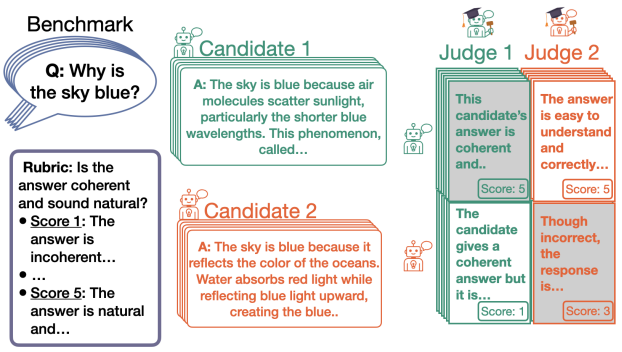

Figure 1: LLM judge workflow: For each benchmark question, LLM judges score each candidate's answer according to a rubric. Candidates are ranked based on their judge-assigned scores. Shaded boxes indicate cases where the same LLM serves as both candidate and judge (self-judging).

ing two questions: (i) from a theoretical standpoint, what are sufficient conditions for an LLM-as-a-judge pipeline to identify the true rankings and (ii) from a methodological standpoint, how can we quantify our confidence in estimated rankings when we do not know if these theoretical conditions hold in practice?

We show that a geometric perspective clarifies the role of epistemic uncertainty and guides both theoretical and methodological development. The key idea is that we can simultaneously visualize judge quality and candidate score distributions on a probability simplex, where geometric concepts (e.g., triangle areas) correspond to key ranking concepts. Epistemic uncertainty manifests as uncertainty in the location of judge points, while aleatoric uncertainty manifests as stochasticity of candidate points. This representation allows us to reason about how the relative positions of these points affect identifiability and estimation of the true rankings.

Using this framework, we find that constancy of LLM judge behavior is sufficient for ranking identifiability in two-level scoring systems. However, this sufficiency breaks down when ranking across three or more levels, uncovering a surprising phase transition. These theoretical results motivate the development of a Bayesian framework for estimating ranks, where we construct minimally-informative geometric priors that encode our prior beliefs about judge quality. We then conduct sensitivity analyses of estimated rankings by varying the strength of the Bayesian priors, which corresponds to varying the level of epistemic uncertainty.

Applying our framework to five LLM benchmark datasets, our sensitivity analyses reveal that estimated candidate rankings are robust in some cases (e.g., GPQA and SummEval) but not others (e.g., Omni-MATH). These results explain the practical success of LLM judges, but also emphasize the importance of their careful, measured use. The Bayesian framework also achieves substantially higher coverage of the true rankings than existing methods, since it captures both aleatoric and epistemic uncertainty whereas standard approaches capture only the former. These results underscore how incorporating epistemic uncertainty is necessary for reliable rankings from LLM judges. Code for reproducing this work and running the Bayesian inference pipeline is available at `https://github.com/jjfenglab/judging-llms-on-a-simplex`.

2 RELATED WORK

LLM-as-a-judge and their implicit assumptions. While LLM judges have emerged as a scalable alternative to traditional metrics that require reference outputs (Papineni et al., 2001; Lin, 2004; Wang et al., 2023; Chiang and Lee, 2023; Li et al., 2024; Gu et al., 2024), current approaches may not fully capture all sources of uncertainty in their rankings. LLM judges exhibit systematic biases such as position bias and verbosity bias (Zheng et al., 2023b; Koo et al., 2024; Wei et al., 2025), echoing known phenomena in human judgment—the halo effect (Thorndike, 1920) and anchoring (Tversky and Kahneman, 1974). Proposed mitigations—score averaging, juries, judge debates, rubrics (Liang et al., 2023; Verga et al., 2024; Kalra and Tang; Chan et al., 2024; Databricks, 2024; Lee et al., 2024)—implicitly assume that judges are perfect or that their errors cancel out in expectation, ignoring uncertainty about judge quality. While Guerdan et al. (2025) discussed the limitations of LLM judges when there is no true agreed-upon rating scale, we prove that even with agreed-upon scales, fundamental identifiability limits exist that no averaging or ensemble method can overcome.

Uncertainty quantification without ground truth. Existing uncertainty quantification methods cannot address the fundamental challenge of epistemic uncertainty about judge quality. Bootstrapping (Goldstein and Spiegelhalter, 1996; Xie et al., 2009) only quantifies sampling variation, leading to undercoverage when assumptions fail. Methods like prediction-powered inference (Chatzi et al., 2024; Angelopoulos et al., 2023), conformal inference (Jung et al., 2025), or consensus models (Raykar et al., 2010; Welinder and Perona, 2010) can integrate LLM judging if some subset of gold-standard labels are available for *each* new model and benchmark, limiting scalability. Bradley-Terry models (Bradley and Terry, 1952; Rao and Kupper, 1967; Herbrich et al., 2006; Ameli et al., 2025), widely used in rating systems like Elo and Chatbot Arena, assume strong stochastic transitivity, restricting their

applicability to settings where pairwise comparisons uniquely determine a global ranking.

Crowdsourcing. A key statistical problem in crowdsourcing is to recover the confusion matrix and impute the true labels for observations given labels from noisy annotators (Dawid and Skene, 1979). This is related to the problem of judging candidates given LLM judges, but a key difference is this work's focus on *ranking* candidates. The ranking perspective allows us to use assumptions that are weaker than those typically considered in the crowdsourcing literature (Welinder and Perona, 2010; Ibrahim et al., 2019).

Imperfect reference standards. Using LLMs as imperfect judges parallels evaluation of medical diagnostics with imperfect reference standards (Reitsma et al., 2009; Umemneku Chikere et al., 2019; Sun and Zhou, 2025; Sun et al., 2024). Our results expand on ideas used in this field, beyond the classical setting of evaluating binary diagnostic tests to the case of multi-level ratings, which are commonly used for LLM evaluation. The geometric arguments substantially extend (Fienberg and Gilbert, 1970; Black and Craig, 2002; Jones et al., 2010; Duan et al., 2020), which focused on identifying diagnostic test performance rather than ranking and only considered the case with binary diagnostic tests.

3 A GEOMETRIC PERSPECTIVE

We study the LLM judge pipeline shown in Figure 1, where J LLM judges score answers by K candidate LLMs to questions from a benchmark task. Formally, denote the spaces of questions and answers as $\mathcal{Q}$ and $\mathcal{A}$, respectively. A benchmark task is defined by a distribution over questions $Q \sim P_{\mathcal{Q}}$ and a true scoring function $s^* : \mathcal{Q} \times \mathcal{A} \to \{1, \dots, M\}$. Each candidate k is a (potentially stochastic) function $f_k : \mathcal{Q} \to \mathcal{A}$ that generates answers, with true score $S_k^* = s^*(Q, f_k(Q))$ for question Q. Candidate k's true score distribution is denoted $\pi_k = (\pi_{k,1}, \dots, \pi_{k,M})$, where $\pi_{k,m} = \Pr(S_k^* = m)$ is the frequency with which the candidate achieves true score m. The goal is to recover the true ranking of candidates with respect to their expected true scores $\mathbb{E}[S_k^*] = \sum_{m=1}^{M} m \cdot \pi_{k,m}$.

We study the setting where both true scoring function s^* and the true scores S_k^* are unobserved. Instead, we rely on the LLM judge pipeline to obtain judge-assigned scores, which can be viewed as noisy proxies. Each judge $j = 1, \cdots, J$ is represented as a function $\hat{s}_j : \mathcal{Q} \times \mathcal{A} \to \{1, \dots, M\}$. So given question Q and candidate k's answer, the judge assigns score $\hat{S}_k^{(j)} = \hat{s}_j(Q, f_k(Q))$. Given infinite questions drawn from the benchmark task, the distribution of judge-assigned scores for candidate k is $\gamma_k^{(j)} = (\gamma_{k,1}^{(j)}, \dots, \gamma_{k,M}^{(j)})$, where $\gamma_{k,m}^{(j)} = \Pr(\hat{S}_k^{(j)} = m)$ is the frequency that judge j assigns score m to the candidate's answers.

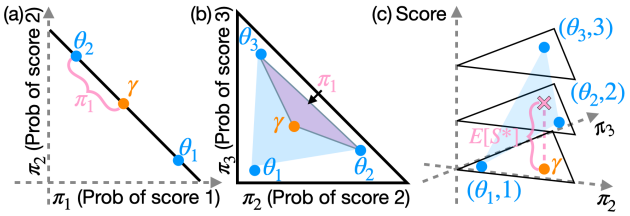

Figure 2: The true prevalence of the true scores corresponds to barycentric coordinates; (a) and (b) highlight prevalence π_1 in 2- and 3-level scoring systems, respectively. A candidate's expected score corresponds to the height of vertical projection in the augmented space, as illustrated in (c).

Using simple geometric arguments, we can relate the true score distribution π_k to the observed score distribution $\gamma_k^{(j)}$ using judge j's confusion matrix for candidate k. In particular, let the mth column of the judge's confusion matrix for candidate k represent the distribution of assigned scores for answers with true score m, i.e.,

$$\theta_{m,k}^{(j)} = \big(\Pr(\hat{S}_k^{(j)} = 1 | S_k^* = m), \dots, \Pr(\hat{S}_k^{(j)} = M | S_k^* = m)\big).$$

Each of the judge's confusion matrix columns $\theta_{m,k}^{(j)}$ for $m = 1, \cdots, M$ lie on the $(M-1)$-dimensional probability simplex and, critically, the candidate's judge-assigned score distribution $\gamma_k^{(j)}$ is the convex combination of these columns with respect to true score distribution, i.e., $\gamma_k^{(j)} = \sum_{m=1}^{M} \pi_{k,m} \theta_{m,k}^{(j)}$. As examples, Figure 2a shows how the judge and candidate in a 2-level scoring system all fall on a line segment and Figure 2b shows how these points in a 3-level scoring system all fall within a triangle. Using this geometric perspective, we can then establish equivalences between geometric concepts to key ranking concepts:

1. True score distributions correspond to barycentric coordinates. π_k corresponds precisely to the *barycentric* coordinates for the weighted centroid $\gamma_k^{(j)}$ relative to judge vertices $\theta_{m,k}^{(j)}$, which are also known as *areal* coordinates because they can be expressed as ratios of simplex sub-areas. For instance, for $M = 3$, $\pi_{k,1}$ equals the area of the subtriangle from the weighted centroid to the 2nd and 3rd vertices divided by the area of the triangle defined by all vertices (Figure 2b), i.e.,

$$\pi_{k,1} = \frac{\text{Area of } \triangle_{(\gamma_k, \theta_2, \theta_3)}}{\text{Area of } \triangle_{(\theta_1, \theta_2, \theta_3)}}, \tag{1}$$

with $\pi_{k,2}$ and $\pi_{k,3}$ defined analogously. This geometric characterization extends to any M.

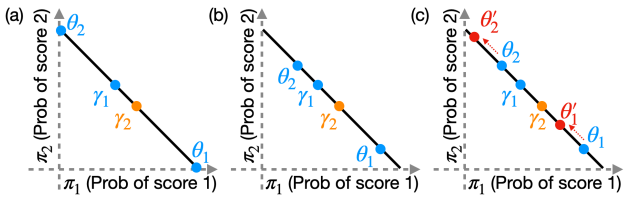

Figure 3: Visualization of judge assumptions for the 2-level scoring setting. We suppose there are two LLMs (1=blue, 2=orange), where both are candidates (with score distributions γ_1 and γ_2) and LLM 1 is a judge. (a) Perfect Judge assumes judge vertices (θ_1, θ_2) are at the extremes of the 1-dimensional probability simplex. (b) Strong Constancy assumes the vertex positions for the judge are same across all candidates. (c) Moderate Constancy assumes the vertex positions for the judge only differ when self-judging (indicated by the red shifted vertices).

2. Expected scores map to height in augmented space. If we augment the probability simplex with an additional axis representing score values and lift each judge vertex $\theta_{m,k}^{(j)}$ to height m, the vertices form an augmented simplex (Figure 2c). Then, as proved in the Appendix, candidate k's expected score $\mathbb{E}[S_k^*]$ corresponds precisely to the height of its vertical projection onto this augmented simplex.

3. Epistemic uncertainty manifests as unknown positions of judge vertices. When multiple configurations of judge vertices are compatible with the observed set of candidate points, the location of the judge vertices cannot be determined. Thus epistemic uncertainty of judge quality is represented by uncertainty in the location of judge vertices.

4. Aleatoric uncertainty manifests as stochasticity of candidate points. Aleatoric uncertainty is sampling variability, which corresponds to us observing the empirical judge-assigned score distributions $\hat{\gamma}_{k,n}^{(j)}$ for a benchmark dataset with n questions, rather than the expected judge-assigned score distribution $\gamma_k^{(j)}$.

4 THEORETICAL LIMITS OF RANKING IDENTIFIABILITY

Using this geometric framework, we now investigate when true rankings can or cannot be recovered from LLM judge scores without ground truth labels. To understand the theoretical limits, we assume access to infinite data samples, resulting in zero aleatoric uncertainty and leaving only epistemic uncertainty. To clarify these limits, we consider assumptions that idealize judge behavior to varying degrees; Section 5 relaxes these idealizations for practical inference.

In the most general case with zero constraints on the LLM judge behaviors, our geometric visualization will have $J \times K \times M$ points representing the performance of the J judges across the K candidates as well as $J \times K$ points representing the score distributions assigned by each judge to each candidate. The true rankings are generally nonidentifiable in this setting, so we must impose structure on judge behavior. Thus we consider assumptions, that when imposed, may sufficiently reduce epistemic uncertainty to make the true rankings identifiable.

The strongest assumption is to assume the judges are perfect. The confusion matrices collapse to the identity matrix, placing all judge vertices at the simplex corners (Figure 3a). If true, this assumption would obviously make the true rankings identifiable for any value of J, M, and/or K. However, this is likely unrealistic.

A weaker and somewhat more realistic assumption is that the judge's performance is perfectly consistent across candidates (*Strong Constancy*). Mathematically, this corresponds to the confusion matrix being the same across candidates, i.e., the vertices for each judge j are shared across candidates (Figure 3b).

Assumption 1 (Strong Constancy)**.** *The confusion matrix of judge j is identical across all K candidates: For each m, there is some $\theta_m^{(j)}$ such that $\theta_{m,k}^{(j)} = \theta_m^{(j)}$ for $k = 1, \cdots, K$.*

A weaker assumption that allows for self-preference bias (Koo et al., 2024) is to suppose that the LLM judge is perfectly consistent as long as it is not judging itself (*Moderate Constancy*). This can be visualized by a separate set of vertices when the LLM is judging itself but a shared set of vertices otherwise (Figure 3c).

Assumption 2 (Moderate Constancy)**.** *Judge $\hat{s}_j$ has an identical confusion matrix for all non-self candidates: For each m, there is some $\theta_m^{(j)}$ such that $\theta_{m,k}^{(j)} = \theta_m^{(j)}$ for all $k \neq j$.*[1]

While one may consider even weaker assumptions, we study the implications of these two constancy conditions on ranking identifiability, as even here the results are nuanced. These theoretical results then motivate our framework in the next section for estimating ranks and quantifying uncertainty.

4.1 2-level scoring systems

Let us consider the simplest setting: a 2-level scoring system with a single judge that satisfies *Strong Constancy*. In this setting, all candidates must lie on the

[1]For simplicity, the theoretical results study the case where self-judging means the same LLM judges itself. In practice, we exclude judges from judging their model family.

line segment between the two judge vertices θ_1 and θ_2. Figure 2 (left) provides a visual proof why the true ranking is identifiable: for 2-level scoring, ranking candidates by expected true score reduces to ranking them by their prevalence of the higher score, which is determined by their order along the line segment. This is true even though we do not know the exact positions of the judge vertices and even if the LLM judges are far from perfect. In fact, our only requirement is that the judges are not adversarial (to avoid the so-called "label-flipping problem" (Sun and Zhou, 2025)), i.e.,

Assumption 3. *Judge j's probability of assigning the lowest score when the true score is equal to m decreases with respect to m.*

For 2-level scoring, this is a weak condition as it only requires the judges to perform better than random.

The result under *Moderate Constancy* is analogous. Using similar geometric reasoning (see Appendix), we find that the only difference is that at least two judges and four candidates are needed to obtain enough information to recover the true ranking.

Theorem 1. *For 2-level scoring, any of the following conditions are sufficient for candidate rankings to be identifiable from the distribution of judge-assigned scores:*

(i) There is $J = 1$ judge and it satisfies Assumptions 1 and 3.
(ii) There are $K \geq 4$ candidates, $J \geq 2$ judges, and the judges satisfy Assumptions 2 and 3.

Remark. For completeness, we present in the Appendix necessary and sufficient conditions for recovering rankings in two-level systems. The geometry is complex, so we defer the details to the appendix.

4.2 3+-level scoring systems

Results for scoring systems with 3 or more levels are qualitatively different. Below, we present geometric arguments for 3-level scoring systems, but the same arguments extend to more levels. To build intuition, we first discuss the tasks of (i) ranking the prevalence of each score and then (ii) ranking the expected scores.

(i) Ranking prevalences. Without loss of generality, suppose we wanted to rank the prevalence of true score $m = 1$. As mentioned in Section 3, this is equivalent to ranking the barycentric coordinates $\pi_{k,1}$ across candidates $k = 1, \cdots, K$, which are defined as the area ratios (1). Under strong constancy, the denominators of these ratios are the same for all k, so ranking $\pi_{k,1}$ reduces to ranking the areas of the subtriangles $\triangle_{(\gamma_k,\theta_2,\theta_3)}$ Nevertheless, we find that the rankings are non-identifiable in general, even under strong constancy. Figure 4 provides a visual proof: panels (a) and (b) show two equally valid judge configurations ($\{\theta_1, \theta_2, \theta_3\}$ versus $\{\theta'_1, \theta'_2, \theta'_3\}$) that can explain candidate score distributions $\gamma_{k=1}$ and $\gamma_{k=2}$, as both judge configurations envelop the candidate points. However, the areas flip between configurations. In panel (a), subtriangle $\triangle_{(\gamma_1,\theta_2,\theta_3)}$ has greater area than $\triangle_{(\gamma_2,\theta_2,\theta_3)}$, while in panel (b) this relationship reverses. Thus the two panels show that even under strong constancy, the rankings of the score prevalences cannot be recovered if there is no prior knowledge about judge quality.

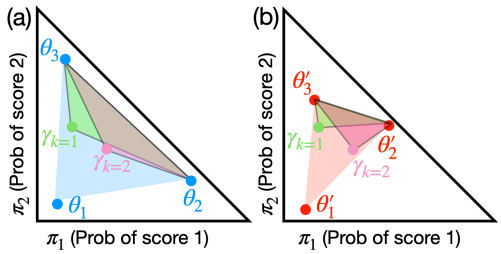

Figure 4: Non-identifiability in 3-level scoring. Same candidate positions (green/pink) explained by different judge configurations yield opposite prevalence rankings: $\pi_{1,1} > \pi_{2,1}$ in (a) vs. $\pi_{1,1} < \pi_{2,1}$ in (b).

(ii) Ranking expected scores. Given the nonidentifiability of prevalence rankings, the ranking of expected true scores is also nonidentifiable without gold standard labels. To see this, recall that each candidate's expected score corresponds to the height of its vertical projection onto the augmented simplex (Figure 2c); these heights change when the judge vertices shift, which can lead to a reordering of candidates. This argument applies under either constancy assumption and for any number of judges.

Together, these results illustrate that epistemic uncertainty can significantly affect recoverability of the true rankings, even when aleatoric uncertainty is removed.

Theorem 2. *Consider the 3+-level scoring setting with all judges either satisfying Assumptions 1 and 3 or Assumptions 2 and 3. Given only the distribution of judge-assigned scores, there exist candidates whose prevalence and/or expected-score rankings cannot be identified.*

4.3 Recoverability is dataset-specific

The prior theoretical results show that recoverability depends not only on judge quality assumptions but also the problem setting. In particular, Theorems 1 and 2 uncover a dependence on the number of scoring levels, supporting the "folk wisdom" that LLM judges tend to be more effective for 2-level scoring systems and less effective for 3+levels (Shankar et al., 2024; Husain,

2025). The geometric perspective further reveals that recoverability is, in fact, dataset-specific, as illustrated in the following two examples. This means we need a way to rigorously quantify how sensitive the estimated rankings for a given dataset are to varying levels of epistemic uncertainty, which we address using Bayesian inference in the next section.

Example 1: Dataset requiring stronger priors. Consider again the Figure 4 example and the task of ranking prevalence of score $m = 1$. Intuitively, the judge configuration in panel (a) may seem more probable than panel (b) if we believe that LLM judges can distinguish scores 2 and 3 moderately well. To formalize this prior belief, we distill it using geometric arguments. In particular, ranking $\pi_{k,1}$ is equivalent to ranking areas of subtriangles $\triangle\gamma_k, \theta_2, \theta_3$. Because all the subtriangles have the same line segment $\overline{\theta_2\theta_3}$ as the base, ranking areas is equivalent to ranking distances from each candidate γ_k to the line $\overleftrightarrow{\theta_2\theta_3}$. Because ranking distances only require knowing the *slope* of this line, it is sufficient to state our prior belief about judge quality in terms of *slopes*. This is something we generally have a good prior about. In contrast, it is generally more difficult to specify one's prior about the exact location of the judge vertices, since LLMs are often miscalibrated (Wang et al., 2024a).

Example 2: Dataset allowing weaker priors. Consider a candidate receiving mostly 1's versus another receiving mostly 3's from an LLM judge (see visualization in Appendix). When score distributions are so different, the ranking between two candidates may be quite evident, even if we have limited prior knowledge on the performance of the LLM judges and even if the constancy assumptions do not hold. However, we need a method to quantify when constancy violations flip rankings, as discussed in the next section.

5 BAYESIAN FRAMEWORK

The theoretical results show that epistemic uncertainty impacts our ability to rank candidates but that the level of impact is dataset-specific. To model this, we design a Bayesian framework that encodes epistemic uncertainty through two priors: (i) how strongly the constancy assumption holds, represented by random effects (Section 5.2), and (ii) prior beliefs about judge discriminative ability, represented by slopes between judge vertices (Section 5.3). We can then conduct sensitivity analyses that assess the ranking robustness to varying levels of epistemic uncertainty, by systematically varying the strength of the Bayesian priors. Moreover, by defining appropriate hyperpriors, we can fully marginalize over our epistemic uncertainty when conducting posterior inference for candidate rankings. We describe the key components of the Bayesian model here; the full specification appears in the Appendix.

5.1 A base probability model

As the base probability model, the assigned score $\hat{S}_{ik}^{(j)}$ by judge j to candidate k's answer to the i-th question, given its true score S_{ik}^*, is modeled as independent draws from a multinomial distribution with parameter $\theta^{(j)}_{S^*_{ik},k}$. Marginalizing out the true latent scores, the likelihood of the observed data is

$$\prod_{i=1}^{n}\prod_{j=1}^{J}\prod_{k\neq j}\Big[\sum_{m=1}^{M}\underbrace{\Pr\left(\hat{S}_{ik}^{(j)}|S_{ik}^*=m;\theta_{m,k}^{(j)}\right)}_{=\theta^{(j)}_{m,k,\hat{S}_{ik}^{(j)}}}\underbrace{\Pr(S_{ik}^*=m)}_{=\pi_{k,m}}\Big],$$

where n is the number of questions. To remove the influence of self-preference, note that we filter for $k \neq j$.

The base model assumes conditional independence given the true score for computational tractability. In practice, residual correlation is still likely, as LLMs are trained on similar datasets. This will be naturally addressed by random effects introduced in the next section, which is motivated from the different angle of relaxing the constancy assumption.

5.2 Prior for relaxing constancy

To relax the constancy assumptions (Assumptions 1 and 2), we model the prevalence of each judge-assigned score for a given candidate using random effects relative to a "base" score prevalence $\vec{\pi}_k$:

$$\vec{\pi}_k^{(j)} = (1 - W_k R_j)\vec{\pi}_k + W_k R_j Z_k$$

where $Z_k \sim \text{Dirichlet}(\delta)$ determines the direction of the deviation, $R_j \sim \text{Beta}(\omega J, J)$ controls the judge-specific magnitude, and $W_k \sim \text{Beta}(\omega K, K)$ controls the candidate-specific magnitude. The hyperparameter $\omega \in [0, \infty)$ controls the degree of constancy violation through the random effect magnitude, where $\omega = 0$ enforces perfect constancy and increasing ω allows progressively larger violations. For instance, $\omega = 1$ expects random effects to contribute half of the effect, while $\omega = 8$ expects a contribution of 90%.

5.3 Prior for varying judge quality

To construct a Bayesian prior over slopes between judge vertices, we parameterize the judge vertices in terms of a weight propagation graph (Figure 5), where each element in the confusion matrix is an average of its parent nodes weighted by edge weights α, i.e., $\theta_{\mathtt{v}}^{(j)} = \sum_{\mathtt{u}\to\mathtt{v}} \theta_{\mathtt{u}}^{(j)} \alpha_{\mathtt{u}\to\mathtt{v}}$. As such, the slopes between

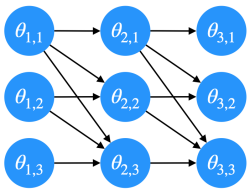

Figure 5: Weight propagation framework for encoding judge quality priors in 3-level scoring, where outgoing edge weights must sum to 1. The probability of the judge assigning score m_2 when the true score is m_1, θ_{m_1,m_2}, equals the weighted sum of all its parent nodes per the incoming edge weights.

vertices are directly controlled in terms of edge weights. This parameterization encodes the prior belief that judges tend to assign scores close to the true score more often than distant ones, while remaining flexible enough to accommodate varying degrees of judge quality. The graph structure also enforces the monotonicity requirement (Assumption 3) by construction. We discuss alternative prior specifications considered in Appendix E.4.

For each node $\mathtt{v}$, we place a Dirichlet prior over the outgoing edge weights $\alpha_{\mathtt{v}}$ indexed by a single hyperparameter $\beta_{\max}$, where increasing $\beta_{\max}$ corresponds to more discriminative judges. For instance, in 3-level scoring, the Dirichlet prior for outgoing edges from node θ_{m_1,m_2} has parameters $\vec{\beta}_{m_1,m_2} = [1, 1+\rho\cdot\beta_{\max}, 1]$ with $\rho \sim \text{Beta}(1,1)$. Full details are in the Appendix.

5.4 Conducting sensitivity analyses

Using this model, we develop a practical protocol for sensitivity analysis to understand how epistemic uncertainty influences confidence in the estimated rankings. In the absence of strong prior knowledge about LLM judge behavior, we recommend the following:

1. Start with conducting Bayesian inference with hyperparameters $\omega = 0$ (perfect constancy) and $\beta_{\max} = 5$ (moderate judge quality).
2. Estimate how rankings shift as the constancy assumption is relaxed, by increasing ω from 0 to 8 while holding $\beta_{\max}$ fixed.
3. Estimate how rankings shift as our prior over judge quality varies, by varying $\beta_{\max}$ from 0 to 20 while holding $\omega = 0$.

If rankings remain stable across parameter variations, the conclusions are reliable despite epistemic uncertainty. Otherwise, one may need to inject additional prior knowledge (e.g., narrow the range of plausible hyperparameter values) or obtain gold-standard labels.

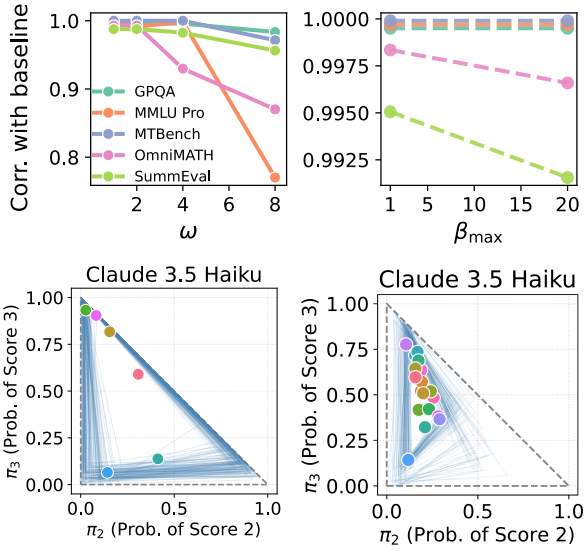

Figure 6: Top: Sensitivity of estimated rankings when varying random effects (RE, left) and judge quality (right) hyperparameters, by plotting the correlation between the estimated ranking for each hyperparameter and their base values ($\omega = 0, \beta_{\max} = 0$). Bottom: Candidates visualized on the probability simplex with judge configurations sampled from posterior (blue triangles), for MTBench (left) and Omni-MATH (right). We collapse 5-level ratings to 3 levels for visualization (see Appendix for mapping details).

6 EXPERIMENTS

Here we present experiments across various LLM benchmarks to assess the impact of epistemic uncertainty on ranking. First, using the geometric Bayesian framework, we conduct sensitivity analyses to determine the robustness of learned rankings. Second, we compare the overall performance of the Bayesian framework to existing methods in terms of coverage and correlation with ground truth rankings. We present our main experimental results below, with ablation studies, implementation details, and extended analyses in the Appendix.

We evaluate the Bayesian framework across three categories of benchmark datasets: **(i) Verifiable tasks with 2-level scores**: GPQA (Rein et al., 2023) and MMLU Pro (Wang et al., 2024b) contain multiple-choice questions graded as correct/incorrect, with judges having an abstention option. **(ii) Multi-level human-judged tasks**: MTBench (Zheng et al., 2023a) evaluates multi-turn conversations while SummEval (Völske et al., 2017) assesses summarizations. Both datasets are assessed on multi-level Likert scales, by LLMs as well as human experts. **(iii) "Semi-verifiable" tasks**: Omni-MATH (Gao et al., 2024) contains mathematical reasoning problems with refer-

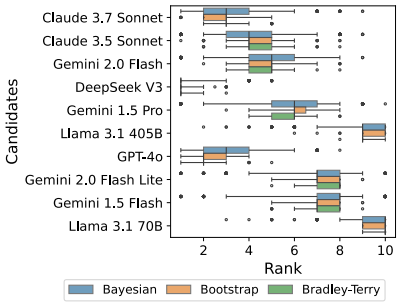

Figure 7: Estimated rankings for the top 10 candidates on GPQA, presented in order by their true rankings. Unlike existing methods, Bayesian method fully incorporates epistemic uncertainty.

ence solutions, though there is no single ground-truth answer. LLM judges are asked to evaluate answers on a 3-level scale (correct, partial credit, incorrect).

We use a two-stage protocol to compare ranking methods. First, LLM judges evaluate candidates without access to ground truth, mirroring real-world usage. Second, we generate ground-truth scores for each answer by comparing against the correct multiple-choice answer on verifiable tasks and obtaining human-assigned scores for human-judged tasks. For semi-verifiable tasks, we rescore each candidate's answer by providing the LLM judge with the provided reference answer. For GPQA, MMLU Pro, and Omni-MATH, we evaluated 19 contemporary models including Claude, GPT, Gemini, Llama, Mistral, and Qwen variants, with Claude 3.5 Haiku and GPT-4o mini serving as judges. These judges were deliberately selected to assess the performance of ranking methods when the judges are imperfect. For MTBench and SummEval, we utilize their existing candidates and judges.

6.1 Sensitivity analyses

For each benchmark dataset, we conducted Bayesian inference with random effects hyperparameter ω values of 0, 1, 2, 4, and 8, corresponding to expected random effect magnitudes of approximately 0, 0.5, 0.7, 0.8, and 0.9 respectively. Figure 6 (left) shows that rankings remain remarkably stable across these variations for most datasets. The correlation between rankings at different ω values and the baseline rankings exceeds 0.95 for GPQA, MTBench, and SummEval, indicating that significant violations of the constancy assumption have minimal impact on the resulting rankings. Similarly, varying the judge quality hyperparameter $\beta_{\max}$ from 1 to 20 produces negligible effects on rankings across all datasets (Figure 6 right), with correlations consistently above 0.99. This insensitivity to the judge quality prior suggests that the observed score data are sufficiently informative to overwhelm the prior on judge discrimination, making the resulting rankings robust to prior beliefs about $\beta_{\max}$. However, both MMLU Pro and Omni-MATH show greater sensitivity to the constancy assumption, with correlations between baseline rankings dropping to 0.77 and 0.86 respectively when ω is increased from 0 to 8. This sensitivity appears pronounced for MMLU Pro for $\omega > 4$, highlighting uncertainty in its rankings because of potential variability in judge performance across candidates.

To understand why estimated rankings are more or less robust, we can visualize the candidates in the probability simplex against possible judge configurations sampled from the posterior distribution of the Bayesian method. Here we compare two contrasting datasets to illustrate why some benchmarks are robust to epistemic uncertainty while others are not. As shown in Figure 6 left, estimated rankings for MTBench are robust even when the constancy assumption is relaxed because (i) candidates are well-separated across the simplex, with clear performance tiers and (ii) the posterior judge configurations are relatively consistent with similar triangular shapes with minimal variability. In contrast, Figure 6 right shows that estimated rankings for Omni-MATH are more sensitive to epistemic uncertainty because (i) candidates cluster tightly in the central region with overlapping score distributions, making their relative ordering sensitive to judge vertex positions, and (ii) the posterior samples demonstrate considerable uncertainty in the judge configurations. Simplex visualizations for MMLU Pro and GPQA are provided in the Appendix.

6.2 Comparative performance evaluation

While Section 6.1 examined ranking estimates qualitatively, this section will evaluate ranking estimates from the Bayesian framework quantitatively, in terms of Spearman correlation between estimated and ground-truth rankings (ranking accuracy) and coverage rate of 95% credible or confidence intervals (calibration). To produce a single point estimate from our Bayesian framework rather than a sensitivity curve, we place hyperpriors over ω and $\beta_{\max}$, integrating out epistemic uncertainty during posterior inference. We compare against the following four baselines: single judge scoring (the score from one LLM judge, without adjudication), simple averaging across multiple judges, bootstrap confidence intervals (Xie et al., 2009), and Bradley-Terry pairwise comparison models (Bradley and Terry, 1952).

The Bayesian framework consistently achieves higher correlations and better coverage across all benchmark datasets (Table 1), with coverage rates improving by over 20 percentage points in some cases. This dramatic improvement in coverage reflects our theoretical find-

Table 1: Ranking method performance on benchmarks in terms of correlation and coverage of ground-truth ranks.

Method	GPQA		MMLU		Omni-MATH		SummEval		MTBench	
	Corr	Cov	Corr	Cov	Corr	Cov	Corr	Cov	Corr	Cov
Bayesian	**0.916** **(0.87, 0.94)**	**0.889** **(0.72, 0.94)**	**0.940** **(0.85, 0.95)**	**1.000** **(0.90, 1.00)**	**0.791** **(0.60, 0.83)**	**0.737** **(0.37, 0.79)**	**0.888** **(0.76, 0.91)**	**0.917** **(0.67, 0.95)**	**1.000** **(0.94, 1.00)**	**1.000** **(1.00, 1.00)**
Bootstrap	0.922 (0.88, 0.93)	0.556 (0.51, 0.83)	0.884 (0.84, 0.90)	0.474 (0.49, 0.68)	0.767 (0.71, 0.80)	0.368 (0.37, 0.47)	0.885 (0.78, 0.90)	0.729 (0.65, 0.96)	0.943 (0.94, 1.00)	1.000 (1.00, 1.00)
Bradley-Terry	0.901 (0.88, 0.92)	0.389 (0.39, 0.67)	0.886 (0.84, 0.90)	0.474 (0.38, 0.58)	0.767 (0.72, 0.79)	0.368 (0.37, 0.42)	0.902 (0.82, 0.91)	0.771 (0.61, 0.91)	0.943 (0.94, 1.00)	1.000 (0.67, 1.00)
Simple Average	0.922 (0.88, 0.93)	0.130 (0.02, 0.28)	0.884 (0.84, 0.90)	0.211 (0.14, 0.28)	0.767 (0.71, 0.80)	0.228 (0.18, 0.33)	0.885 (0.78, 0.90)	0.271 (0.09, 0.54)	0.943 (0.94, 1.00)	0.667 (0.67, 1.00)
Single Judge	0.869 (0.81, 0.90)	0.130 (0.02, 0.28)	0.855 (0.81, 0.89)	0.211 (0.14, 0.28)	0.725 (0.70, 0.75)	0.228 (0.18, 0.33)	0.787 (0.58, 0.86)	0.285 (0.06, 0.45)	0.971 (0.94, 1.00)	0.833 (0.67, 1.00)

ing that epistemic uncertainty is essential for proper uncertainty quantification. The correlation improvements, while more modest, demonstrate that incorporating judge uncertainty also benefits ranking estimates. Figure 7 illustrates how this coverage improvement is achieved: as seen on the GPQA dataset, the intervals from Bayesian inference are indeed significantly wider than those produced by comparator methods. These wider intervals reflect genuine epistemic uncertainty about judge quality. Baseline methods produce narrower intervals by treating judge parameters as known, which leads to systematic undercoverage when those assumptions are violated (Table 1). Conversely, credible intervals that are narrow represent areas of low posterior uncertainty, which can occur due to the discrete nature of ranks as well as the consistency in ranks assigned by judges. Posterior distributions for the other datasets are given in the Appendix.

7 DISCUSSION

This work presents a geometric framework for understanding when gold-standard rankings can and cannot be recovered from only scores assigned by imperfect LLM judges and not gold-standard scores. By representing judges and candidates on a probability simplex, we establish theoretical conditions for ranking identifiability and develop a sensitivity analysis approach. Our key conclusion is that epistemic uncertainty about judge quality critically affects ranking reliability and is not captured by existing methods. The geometric perspective reveals that identifiability depends on scoring levels, judge consistency, and candidate separation in the simplex.

Future work includes deriving formal guarantees on the maximum achievable ranking accuracy given judge quality constraints, and extending the framework to more diverse judge ensembles and scoring rubrics. In addition, the Bayesian framework can be readily extended to incorporate gold-standard labels when they are available, as a Bayesian extension of methods like prediction-powered inference (Angelopoulos et al., 2023). Finally, more work can be done to understand the tradeoffs between different methods for improving ranking estimates, such as through statistical correction in this work versus the collection of a small set of gold-standard scores; we include basic experiments comparing the two options in the Appendix.

ACKNOWLEDGMENTS

J.F. and P.V. were supported through a Patient-Centered Outcomes Research Institute® (PCORI®) Award (ME-2022C1-25619). The authors thank Gene Pennello and Nicholas Petrick (U.S. Food and Drug Administration, Center for Devices and Radiological Health) for helpful discussions.

References

Siavash Ameli, Siyuan Zhuang, Ion Stoica, and Michael W Mahoney. A statistical framework for ranking LLM-based chatbots. In *The Thirteenth International Conference on Learning Representations*, 2025.

Anastasios N Angelopoulos, Stephen Bates, Clara Fannjiang, Michael I Jordan, and Tijana Zrnic. Prediction-powered inference. *Science*, 382(6671): 669–674, November 2023.

Michael A Black and Bruce A Craig. Estimating disease prevalence in the absence of a gold standard. *Stat. Med.*, 21(18):2653–2669, September 2002.

Ralph Allan Bradley and Milton E Terry. Rank analysis of incomplete block designs: I. the method of paired comparisons. *Biometrika*, 39(3/4):324, December 1952.

Chi-Min Chan, Weize Chen, Yusheng Su, Jianxuan Yu, Wei Xue, Shanghang Zhang, Jie Fu, and Zhiyuan Liu. ChatEval: Towards better LLM-based evaluators through multi-agent debate. In *The Twelfth International Conference on Learning Representations*, 2024.

Ivi Chatzi, Eleni Straitouri, Suhas Thejaswi, and Manuel Gomez Rodriguez. Prediction-powered ranking of large language models. In *The Thirty-eighth*

Annual Conference on Neural Information Processing Systems, November 2024.

Cheng-Han Chiang and Hung-Yi Lee. Can large language models be an alternative to human evaluations? *Annual Meeting of the Association for Computational Linguistics*, pages 15607–15631, May 2023.

Databricks. Enhancing LLM-as-a-judge with grading notes. `https://www.databricks.com/blog/enhancing-llm-as-a-judge-with-grading-notes`, July 2024. Accessed: 2025-2-14.

A P Dawid and A M Skene. Maximum likelihood estimation of observer error-rates using the EM algorithm. *J. R. Stat. Soc. Ser. C. Appl. Stat.*, 28(1): 20, 1979.

Rui Duan, Ming Cao, Yang Ning, Mingfu Zhu, Bin Zhang, Aidan McDermott, Haitao Chu, Xiaohua Zhou, Jason H Moore, Joseph G Ibrahim, Daniel O Scharfstein, and Yong Chen. Global identifiability of latent class models with applications to diagnostic test accuracy studies: A gröbner basis approach. *Biometrics*, 76(1):98–108, March 2020.

Stephen E Fienberg and John P Gilbert. The geometry of a two by two contingency table. *J. Am. Stat. Assoc.*, 65(330):694–701, June 1970.

Bofei Gao, Feifan Song, Zhe Yang, Zefan Cai, Yibo Miao, Qingxiu Dong, Lei Li, Chenghao Ma, Liang Chen, Runxin Xu, Zhengyang Tang, Benyou Wang, Daoguang Zan, Shanghaoran Quan, Ge Zhang, Lei Sha, Yichang Zhang, Xuancheng Ren, Tianyu Liu, and Baobao Chang. Omni-MATH: A universal olympiad level mathematic benchmark for large language models. In *The Thirteenth International Conference on Learning Representations*, October 2024.

Harvey Goldstein and David J Spiegelhalter. League tables and their limitations: Statistical issues in comparisons of institutional performance. *J. R. Stat. Soc. Ser. A Stat. Soc.*, 159(3):385, 1996.

Jiawei Gu, Xuhui Jiang, Zhichao Shi, Hexiang Tan, Xuehao Zhai, Chengjin Xu, Wei Li, Yinghan Shen, Shengjie Ma, Honghao Liu, Yuanzhuo Wang, and Jian Guo. A survey on LLM-as-a-judge. *arXiv [cs.CL]*, November 2024.

Luke Guerdan, Solon Barocas, Kenneth Holstein, Hanna Wallach, Zhiwei Steven Wu, and Alexandra Chouldechova. Validating LLM-as-a-judge systems in the absence of gold labels. *arXiv [cs.LG]*, March 2025.

Ralf Herbrich, Tom Minka, and Thore Graepel. TrueSkill™: A bayesian skill rating system. *Advances in Neural Information Processing Systems*, 19, 2006.

Hamel Husain. A field guide to rapidly improving AI products. `https://www.oreilly.com/radar/a-field-guide-to-rapidly-improving-ai-products/`, April 2025. Accessed: 2025-9-18.

Shahana Ibrahim, Xiao Fu, Nikos Kargas, and Kejun Huang. Crowdsourcing via pairwise co-occurrences: Identifiability and algorithms. *Adv. Neural Inf. Process. Syst.*, September 2019.

Geoffrey Jones, Wesley O Johnson, Timothy E Hanson, and Ronald Christensen. Identifiability of models for multiple diagnostic testing in the absence of a gold standard. *Biometrics*, 66(3):855–863, September 2010.

Jaehun Jung, Faeze Brahman, and Yejin Choi. Trust or escalate: LLM judges with provable guarantees for human agreement. In *The Thirteenth International Conference on Learning Representations*, 2025.

Nimit Kalra and Leonard Tang. VERDICT: A library for compound LLM judge systems.

Ryan Koo, Minhwa Lee, Vipul Raheja, Jong Inn Park, Zae Myung Kim, and Dongyeop Kang. Benchmarking cognitive biases in large language models as evaluators. In *Findings of the Association for Computational Linguistics ACL 2024*, pages 517–545, Stroudsburg, PA, USA, 2024. Association for Computational Linguistics.

Yukyung Lee, Joonghoon Kim, Jaehee Kim, Hyowon Cho, and Pilsung Kang. CheckEval: Robust evaluation framework using large language model via checklist. *arXiv [cs.CL]*, March 2024.

Dawei Li, Bohan Jiang, Liangjie Huang, Alimohammad Beigi, Chengshuai Zhao, Zhen Tan, Amrita Bhattacharjee, Yuxuan Jiang, Canyu Chen, Tianhao Wu, Kai Shu, Lu Cheng, and Huan Liu. From generation to judgment: Opportunities and challenges of LLM-as-a-judge. *arXiv [cs.AI]*, November 2024.

Percy Liang, Rishi Bommasani, Tony Lee, Dimitris Tsipras, Dilara Soylu, Michihiro Yasunaga, Yian Zhang, Deepak Narayanan, Yuhuai Wu, Ananya Kumar, Benjamin Newman, Binhang Yuan, Bobby Yan, Ce Zhang, Christian Alexander Cosgrove, Christopher D Manning, Christopher Re, Diana Acosta-Navas, Drew Arad Hudson, Eric Zelikman, Esin Durmus, Faisal Ladhak, Frieda Rong, Hongyu Ren, Huaxiu Yao, Jue Wang, Keshav Santhanam, Laurel Orr, Lucia Zheng, Mert Yuksekgonul, Mirac Suzgun, Nathan Kim, Neel Guha, Niladri S Chatterji, Omar Khattab, Peter Henderson, Qian Huang, Ryan Andrew Chi, Sang Michael Xie, Shibani Santurkar, Surya Ganguli, Tatsunori Hashimoto, Thomas Icard, Tianyi Zhang, Vishrav Chaudhary, William Wang, Xuechen Li, Yifan Mai, Yuhui Zhang, and Yuta Koreeda. Holistic evaluation of language models. *Transactions on Machine Learning Research*, February 2023.

Chin-Yew Lin. ROUGE: A package for automatic evaluation of summaries. In *Text Summarization Branches Out*, pages 74–81, 2004.

Kishore Papineni, Salim Roukos, Todd Ward, and Wei-Jing Zhu. BLEU: a method for automatic evaluation of machine translation. In *Proceedings of the 40th Annual Meeting on Association for Computational Linguistics - ACL '02*, Morristown, NJ, USA, 2001. Association for Computational Linguistics.

P V Rao and L L Kupper. Ties in paired-comparison experiments: A generalization of the bradley-terry model. *J. Am. Stat. Assoc.*, 62(317):194, March 1967.

V Raykar, Shipeng Yu, Linda H Zhao, G Hermosillo, Charles Florin, L Bogoni, and Linda Moy. Learning from crowds. *J. Mach. Learn. Res.*, 11(43):1297–1322, March 2010.

David Rein, Betty Li Hou, Asa Cooper Stickland, Jackson Petty, Richard Yuanzhe Pang, Julien Dirani, Julian Michael, and Samuel R Bowman. GPQA: A graduate-level google-proof Q&A benchmark. *arXiv [cs.AI]*, November 2023.

Johannes B Reitsma, Anne W S Rutjes, Khalid S Khan, Arri Coomarasamy, and Patrick M Bossuyt. A review of solutions for diagnostic accuracy studies with an imperfect or missing reference standard. *J. Clin. Epidemiol.*, 62(8):797–806, August 2009.

Shreya Shankar, J D Zamfirescu-Pereira, Bjoern Hartmann, Aditya Parameswaran, and Ian Arawjo. Who validates the validators? aligning LLM-assisted evaluation of LLM outputs with human preferences. In *Proceedings of the 37th Annual ACM Symposium on User Interface Software and Technology*, volume 4, pages 1–14, New York, NY, USA, October 2024. ACM.

Ao Sun and Xiao-Hua Zhou. Estimation of diagnostic test accuracy without gold standards. *Stat. Med.*, 44 (3-4):e10315, February 2025.

Jiarui Sun, Chao Tang, Wuxiang Xie, and Xiao-Hua Zhou. Nonparametric receiver operating characteristic curve analysis with an imperfect gold standard. *Biometrics*, 80(3):ujae063, July 2024.

Edward L Thorndike. A constant error in psychological ratings. *J. Appl. Psychol.*, 4(1):25–29, 1920.

Amos Tversky and Daniel Kahneman. Judgment under uncertainty: Heuristics and biases. *Science*, 185 (4157):1124–1131, 1974.

Chinyereugo M Umemneku Chikere, Kevin Wilson, Sara Graziadio, Luke Vale, and A Joy Allen. Diagnostic test evaluation methodology: A systematic review of methods employed to evaluate diagnostic tests in the absence of gold standard - an update. *PLoS One*, 14(10):e0223832, October 2019.

Pat Verga, Sebastian Hofstatter, Sophia Althammer, Yixuan Su, Aleksandra Piktus, Arkady Arkhangorodsky, Minjie Xu, Naomi White, and Patrick Lewis. Replacing judges with juries: Evaluating LLM generations with a panel of diverse models. *arXiv [cs.CL]*, April 2024.

Michael Völske, Martin Potthast, Shahbaz Syed, and Benno Stein. TL;DR: Mining reddit to learn automatic summarization. In Lu Wang, Jackie Chi Kit Cheung, Giuseppe Carenini, and Fei Liu, editors, *Proceedings of the Workshop on New Frontiers in Summarization*, pages 59–63, Stroudsburg, PA, USA, 2017. Association for Computational Linguistics.

Peiyi Wang, Lei Li, Liang Chen, Zefan Cai, Dawei Zhu, Binghuai Lin, Yunbo Cao, Lingpeng Kong, Qi Liu, Tianyu Liu, and Zhifang Sui. Large language models are not fair evaluators. In Lun-Wei Ku, Andre Martins, and Vivek Srikumar, editors, *Proceedings of the 62nd Annual Meeting of the Association for Computational Linguistics (Volume 1: Long Papers)*, pages 9440–9450, Stroudsburg, PA, USA, 2024a. Association for Computational Linguistics.

Yidong Wang, Zhuohao Yu, Zhengran Zeng, Linyi Yang, Cunxiang Wang, Hao Chen, Chaoya Jiang, Rui Xie, Jindong Wang, Xing Xie, Wei Ye, Shikun Zhang, and Yue Zhang. PandaLM: An automatic evaluation benchmark for LLM instruction tuning optimization. *arXiv [cs.CL]*, June 2023.

Yubo Wang, Xueguang Ma, Ge Zhang, Yuansheng Ni, Abhranil Chandra, Shiguang Guo, Weiming Ren, Aaran Arulraj, Xuan He, Ziyan Jiang, Tianle Li, Max Ku, Kai Wang, Alex Zhuang, Rongqi Fan, Xiang Yue, and Wenhu Chen. MMLU-pro: A more robust and challenging multi-task language understanding benchmark. *arXiv [cs.CL]*, June 2024b.

Hui Wei, Shenghua He, Tian Xia, Fei Liu, Andy Wong, Jingyang Lin, and Mei Han. Systematic evaluation of LLM-as-a-judge in LLM alignment tasks: Explainable metrics and diverse prompt templates. In *ICLR 2025 Workshop on Building Trust in Language Models and Applications*, March 2025.

Peter Welinder and Pietro Perona. Online crowdsourcing: Rating annotators and obtaining cost-effective labels. In *2010 IEEE Computer Society Conference on Computer Vision and Pattern Recognition - Workshops*, pages 25–32. IEEE, June 2010.

Minge Xie, Kesar Singh, and Cun-Hui Zhang. Confidence intervals for population ranks in the presence of ties and near ties. *J. Am. Stat. Assoc.*, 104(486): 775–788, June 2009.

Lianmin Zheng, Wei-Lin Chiang, Ying Sheng, Siyuan Zhuang, Zhanghao Wu, Yonghao Zhuang, Zi Lin, Zhuohan Li, Dacheng Li, E Xing, Haotong Zhang,

Joseph E Gonzalez, and Ion Stoica. Judging LLM-as-a-judge with MT-bench and chatbot arena. *Neural Inf Process Syst*, abs/2306.05685, June 2023a.

Lianmin Zheng, Wei-Lin Chiang, Ying Sheng, Siyuan Zhuang, Zhanghao Wu, Yonghao Zhuang, Zi Lin, Zhuohan Li, Dacheng Li, Eric Xing, Hao Zhang, Joseph E Gonzalez, and Ion Stoica. Judging LLM-as-a-judge with MT-bench and chatbot arena. In *Thirty-seventh Conference on Neural Information Processing Systems Datasets and Benchmarks Track*, November 2023b.

Checklist

1. For all models and algorithms presented, check if you include:
   (a) A clear description of the mathematical setting, assumptions, algorithm, and/or model. [Yes] Sections 3-5
   (b) An analysis of the properties and complexity (time, space, sample size) of any algorithm. [Yes]
   (c) (Optional) Anonymized source code, with specification of all dependencies, including external libraries. [Yes] URL in introduction section.

2. For any theoretical claim, check if you include:
   (a) Statements of the full set of assumptions of all theoretical results. [Yes] Section 4
   (b) Complete proofs of all theoretical results. [Yes] Statements of proofs in Section 4, proofs in supplement.
   (c) Clear explanations of any assumptions. [Yes]

3. For all figures and tables that present empirical results, check if you include:
   (a) The code, data, and instructions needed to reproduce the main experimental results (either in the supplemental material or as a URL). [Yes] URL in introduction
   (b) All the training details (e.g., data splits, hyperparameters, how they were chosen). [Yes]
   (c) A clear definition of the specific measure or statistics and error bars (e.g., with respect to the random seed after running experiments multiple times). [Yes]
   (d) A description of the computing infrastructure used. (e.g., type of GPUs, internal cluster, or cloud provider). [Yes] The Bayesian method runs on a consumer laptop, we explain this in the supplement.

4. If you are using existing assets (e.g., code, data, models) or curating/releasing new assets, check if you include:
   (a) Citations of the creator If your work uses existing assets. [Yes] We cite the benchmark datasets we use in our experiments
   (b) The license information of the assets, if applicable. [Not Applicable]
   (c) New assets either in the supplemental material or as a URL, if applicable. [Not Applicable]
   (d) Information about consent from data providers/curators. [Not Applicable]

(e) Discussion of sensible content if applicable, e.g., personally identifiable information or offensive content. [Not Applicable]

5. If you used crowdsourcing or conducted research with human subjects, check if you include:
   (a) The full text of instructions given to participants and screenshots. [Not Applicable]
   (b) Descriptions of potential participant risks, with links to Institutional Review Board (IRB) approvals if applicable. [Not Applicable]
   (c) The estimated hourly wage paid to participants and the total amount spent on participant compensation. [Not Applicable]

LLMs Judging LLMs: A Simplex Perspective
Supplementary Materials

A GEOMETRIC PERSPECTIVE: ADDITIONAL DETAILS

A.1 Expected scores map to height in augmented space

A key geometric insight used throughout the analysis is that a candidate's expected score corresponds to its height when the probability simplex is embedded in a higher-dimensional space. This result connects the abstract barycentric coordinates to the ranking task.

Theorem 3 (Height Correspondence in Augmented Simplex)**.** *Consider embedding the $(M-1)$-dimensional probability simplex into M-dimensional space by adding a "score" axis. Lift each judge vertex $\theta_m^{(j)}$ to position $(\theta_m^{(j)}, m)$, placing it at height m. For any candidate k with barycentric coordinates $\vec{\pi}_k = (\pi_{k,1}, \ldots, \pi_{k,M})$, when positioned in the augmented space using these same coordinates, its height equals its expected score $\mathbb{E}[S_k^*]$.*

Proof. The candidate's position in the original $(M-1)$-dimensional simplex is determined by its barycentric coordinates:

$$\gamma_k^{(j)} = \sum_{m=1}^{M} \pi_{k,m} \theta_m^{(j)} \tag{A.1}$$

where $\pi_{k,m}$ represents the weight given to judge vertex $\theta_m^{(j)}$.

To augment the space, the simplex is embedded into M-dimensional space by adding a "score" coordinate. Each judge vertex $\theta_m^{(j)}$ is lifted to position $(\theta_m^{(j)}, m)$, placing it at height equal to its score value m.

When the candidate is positioned in this augmented space using the same barycentric coordinates $\pi_{k,m}$, the result is:

$$\text{Augmented position} = \sum_{m=1}^{M} \pi_{k,m} \left(\theta_m^{(j)}, m\right) \tag{A.2}$$

This convex combination gives:

- Simplex coordinates: $\gamma_k^{(j)} = \sum_{m=1}^{M} \pi_{k,m} \theta_m^{(j)}$ (unchanged)
- Height coordinate: $h_k = \sum_{m=1}^{M} \pi_{k,m} \cdot m$

The height $h_k = \sum_{m=1}^{M} \pi_{k,m} \cdot m$ is precisely the definition of the expected score $\mathbb{E}[S_k^*]$, where $\pi_{k,m} = \Pr(S_k^* = m)$.

Thus, the candidate's height in the augmented space directly encodes its expected score, so ranking candidates reduces to comparing their heights. □

This geometric correspondence means that candidates automatically acquire heights equal to their expected scores when the simplex is embedded in augmented space using the barycentric coordinates. Ranking then reduces to comparing heights. This representation also captures how uncertainty in judge vertex positions (epistemic uncertainty) translates to uncertainty in candidate heights and thus rankings.

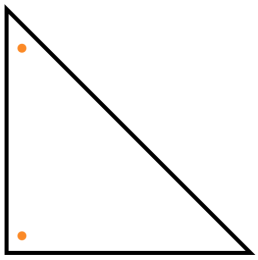

Figure A.1: Example where candidate rankings are likely identifiable even when there are 3+ levels, due to characteristics of the dataset. Candidates have assigned scores that are very different (mostly 1's versus mostly 3's).

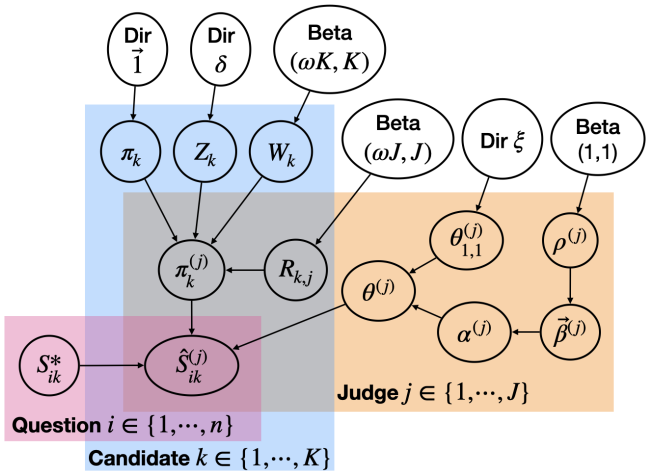

Figure B.2: Plate diagram of the Bayesian model

A.2 Recoverability is dataset-specific

Special cases exist where rankings are robust to judge quality assumptions despite the general non-identifiability result for 3+-level scoring systems. When candidates have substantially different score distributions—manifesting as widely separated points on the probability simplex—their relative ordering remains stable across a broad range of plausible judge configurations. See Figure A.1 as an example (Example 2 in Section 4.3).

B BAYESIAN MODEL

B.1 Probability Model

For judge j evaluating candidate k's answer to the i-th question, the assigned score $\hat{S}_{ik}^{(j)}$ given its true score S_{ik}^* is assumed to follow a multinomial distribution with parameter $\theta_{S_{ik}^*,k}^{(j)}$ (Figure B.2). To keep the model tractable while preserving the geometric structure from Section 3, conditional independence across judges and questions is assumed. After marginalizing over the true latent scores, the likelihood of the observed data becomes:

$$\prod_{i=1}^{n}\prod_{j=1}^{J}\prod_{k\neq j}\Big[\sum_{m=1}^{M}\underbrace{\Pr\left(\hat{S}_{ik}^{(j)}|S_{ik}^*=m;\theta_{m,k}^{(j)}\right)}_{=\theta^{(j)}_{m,k,\hat{S}_{ik}^{(j)}}}\underbrace{\Pr(S_{ik}^*=m)}_{=\pi_{k,m}}\Big], \tag{B.3}$$

where n is the number of questions and self-evaluations ($k \neq j$) are excluded to avoid self-preference bias.

Although judge scores are likely correlated in practice and (B.3) simplifies the true data-generating mechanism, modeling the full joint distribution would add complexity and require additional constancy assumptions without

changing the identifiability results in Section 3. For binary scoring systems, posterior inference under this model yields consistent estimators for prevalences and rankings even when correlation structure is ignored.

B.2 Random Effects Parameterization

B.2.1 Complete Hierarchical Specification

To relax the constancy assumption while keeping the model tractable, random effects are introduced that allow judge-specific and candidate-specific deviations from base prevalences. The complete hierarchical model is:

$$Z_k \sim \text{Dirichlet}(\delta) \quad \text{(candidate-specific random direction)} \tag{B.4}$$

$$R_j \sim \text{Beta}(\omega J, J) \quad \text{(judge-specific random effect magnitude)} \tag{B.5}$$

$$W_k \sim \text{Beta}(\omega K, K) \quad \text{(candidate-specific random effect magnitude)} \tag{B.6}$$

$$\vec{\pi}_k^{(j)} = (1 - W_k R_j)\vec{\pi}_k + W_k R_j Z_k \quad \text{(perturbed prevalences)} \tag{B.7}$$

The perturbed prevalences $\vec{\pi}_k^{(j)}$ replace $\vec{\pi}_k$ in the likelihood (B.3). This parameterization ensures that $\vec{\pi}_k^{(j)}$ remains on the probability simplex for all valid parameter values.

B.2.2 Choice of Prevalence vs. Confusion Matrix Perturbation

Two approaches for introducing random effects were considered: perturbations in judge performance (i.e. $\theta_{m,k}^{(j)}$ as perturbations of $\theta_m^{(j)}$) or in score prevalences (i.e. $\vec{\pi}_k^{(j)}$ as perturbations of $\vec{\pi}_k$).

Prevalence perturbation was chosen for several reasons. For M-level scoring with J judges and K candidates, confusion matrix perturbation requires $O(JKM^2)$ parameters while prevalence perturbation requires only $O(JKM)$. Fewer parameters reduce the risk of overfitting and model misspecification and enable faster MCMC convergence. Deviations in prevalences also correspond directly to changes in perceived candidate quality across judges.

B.2.3 Setting δ for Detecting Specific Biases

The Dirichlet parameter δ controls the distribution of random directions and can be tuned to detect specific types of bias:

- Uniform exploration: $\delta = [1, 1, ..., 1]$ explores all directions equally
- Score inflation detection: For 3-level scoring, $\delta = [1, 4, 10]$ places more weight on higher scores, detecting judges who systematically overrate candidates
- Score deflation detection: For 3-level scoring, $\delta = [10, 4, 1]$ places more weight on lower scores, detecting overly critical judges
- Central tendency bias: $\delta = [1, 10, 1]$ for 3-level scoring detects judges who avoid extreme scores

In the experiments, score inflation detection ($\delta = [1, 4, 10]$) is used because self-preference bias typically manifests as inflated scores for one's own model family.

B.3 Judge Quality Prior Specification

The judge quality prior is implemented through a transition weight framework that parameterizes the confusion matrix columns (judge vertices) as weighted combinations of base positions. This section provides the full mathematical specification of the framework briefly introduced in Section 5.3 of the main paper. This approach encodes beliefs about relative vertex positions while maintaining the probabilistic constraints of the confusion matrix.

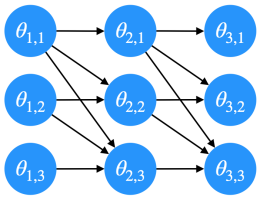

$$\left\{\alpha_{(m_1,m_2)\to(m_1',m_2')}\right\}_{(m_1',m_2') \text{ s.t. } (m_1,m_2)\to(m_1',m_2')} \sim \text{Dirichlet}(\vec{\beta}_{(m_1,m_2)})$$
$$\theta^{(j)}_{m_1',m_2'} = \sum_{(m_1,m_2)\to(m_1',m_2')} \theta^{(j)}_{(m_1,m_2)} \alpha_{(m_1,m_2)\to(m_1',m_2')}$$

Figure B.3: Transition weight framework for encoding judge quality priors in 3-level scoring. Nodes represent pairs (m_1, m_2) where m_1 is the true score and m_2 is the assigned score. Edges show allowed transitions, with weights α drawn from Dirichlet priors parameterized by $\vec{\beta}_{(m_1,m_2)}$ (see Appendix B.3 for formal specification).

B.3.1 Transition Weight Framework

The judge's confusion matrix columns (vertices) are parameterized through a directed acyclic graph where nodes represent confusion matrix entries and edges control how probability mass flows between them. Prior beliefs about judge quality are encoded through the edge weights while ensuring mathematical constraints are satisfied.

The formal specification of the transition weights is:

$$\left\{\alpha_{(m_1,m_2)\to(m_1',m_2')}\right\}_{(m_1',m_2') \text{ s.t. } (m_1,m_2)\to(m_1',m_2')} \sim \text{Dirichlet}(\vec{\beta}_{(m_1,m_2)})$$
$$\theta^{(j)}_{m_1',m_2'} = \sum_{(m_1,m_2)\to(m_1',m_2')} \theta^{(j)}_{(m_1,m_2)} \alpha_{(m_1,m_2)\to(m_1',m_2')}$$

Each node (m_1, m_2) in the transition graph represents a confusion matrix entry: the probability of assigning score m_2 when the true score is m_1. The transition weights $\alpha_{(m_1,m_2)\to(m_1',m_2')}$ control how probability mass flows from parent to child nodes. All outgoing weights from any parent node sum to one, ensuring the result remains a valid probability distribution. The final confusion matrix entry $\theta^{(j)}_{m_1',m_2'}$ for judge j is a weighted average of its parent nodes' values, weighted by the incoming edge weights.

For example, in Figure B.3, the probability $\theta_{2,2}$ (assigning score 2 when true score is 2) receives contributions from both $\theta_{1,1}$ and $\theta_{1,2}$ through their respective edge weights.

B.3.2 Parameterization for 3-Level Scoring

For a 3-level scoring system, the Dirichlet parameters $\vec{\beta}_{(m_1,m_2)}$ are specified as follows:

$$\begin{aligned}
\vec{\beta}^{(j)}_{1,1} &= [1, 1 + \rho^{(j)}\beta_{\max}, 1] \\
\vec{\beta}^{(j)}_{1,2} &= [\beta^{(j)}_{1,1,2}, \beta^{(j)}_{1,1,3}] \\
\vec{\beta}^{(j)}_{2,1} &= [1, 1, 1 + \rho^{(j)}\beta_{\max}] \\
\vec{\beta}^{(j)}_{2,2} &= [\beta^{(j)}_{2,1,2}, \beta^{(j)}_{2,1,3}],
\end{aligned}$$

where:

- $\beta_{\max}$ is the global hyperparameter controlling prior strength about judge quality
- $\rho^{(j)} \sim \text{Beta}(1, 1)$ allows judge-specific variation in discrimination ability (drawn from a uniform hyperprior on $[0, 1]$)
- The structure ensures higher weight on correct identification (diagonal elements) as $\beta_{\max}$ increases

Note that $\alpha_{1,3}$ and $\alpha_{2,3}$ are deterministically set equal to one as these represent terminal nodes in the transition graph with no outgoing edges.

Intuitively, when $\beta_{\max} = 0$, all Dirichlet parameters equal 1 (uniform prior), allowing maximum flexibility in judge behavior. As $\beta_{\max}$ increases, the parameters $[1, 1 + \rho^{(j)}\beta_{\max}, 1]$ place more weight on the middle transition, encoding our belief that better judges more consistently assign higher scores when the true score increases.

B.3.3 Enforcing Monotonicity Through Graph Structure

The transition graph topology automatically enforces Assumption 3 (monotonicity) by restricting which edges exist. Specifically, edges from node (m_1, m_2) to (m_1', m_2') only exist when:

- $m_1' = m_1 + 1$ (moving to the next true score level)
- $m_2' \geq m_2$ (assigned score cannot decrease as true score increases)

This structural constraint ensures that judges cannot be "label-flippers" who systematically assign lower scores to better answers, without requiring explicit inequality constraints during MCMC sampling.

B.3.4 Extension to M-Level Scoring

For general M-level scoring systems, the framework extends naturally:

- The graph has $M(M+1)/2$ nodes representing all valid (m_1, m_2) pairs where $m_2 \geq m_1$
- Edge constraints follow the same monotonicity rules
- Dirichlet parameters follow the pattern: higher values along paths that preserve or increase the assigned score relative to the true score

The parameterization for $M > 3$ follows similar principles, with $\beta_{\max}$ controlling the concentration around correct identification. The accompanying code provides exact implementation details for different values of M.

C IMPLEMENTATION DETAILS

Bayesian inference: Posterior inference is conducted using Hamiltonian Monte Carlo (HMC) in Stan (Stan Development Team, 2021). HMC ran with 4 chains, each with 1000 warmup iterations and 1000 sampling iterations.

Abstention: In practice, the judge may not always be sure what score to assign. The judge is given the option to abstain when there are only two levels, e.g. correct or not.

D EXPERIMENT CONFIGURATION

D.1 Benchmarks

- **GPQA** (Rein et al., 2023): Questions resistant to simple internet searches across STEM domains, stratified by difficulty (undergraduate, graduate, post-graduate).
- **MMLU Pro** (Wang et al., 2024): Enhanced professional knowledge questions across 16 domain-specific subcategories from natural sciences, social sciences, and humanities.
- **MTBench** (Zheng et al., 2023): A conversational benchmark evaluating single- and multi-turn dialogue capabilities across diverse scenarios (creative writing, reasoning, coding, mathematics, role-playing). Human judges rated responses on a 10-point scale. LLM judges are asked for ratings on a simplified 5-point scale.
- **TLDR** (aka SummEval) (Fabbri et al., 2021): A summarization benchmark where models condense news articles into concise summaries, with human ratings across four dimensions (relevance, consistency, fluency, coherence) on 5-point scales.
- **Omni-MATH** (Gao et al., 2024): A benchmark of competition-level problems from International and National Olympiads. These problems are difficult to evaluate automatically because solutions vary in approach, notation, and presentation; multiple valid solution paths may exist; and partial correctness must be assessed along multiple dimensions.

D.2 LLM judges

Two LLM judges are used: Claude 3.5 Haiku (anthropic/claude-3-5-haiku-20241022) and GPT-4o Mini (gpt-4o-mini-2024-07-18) for all benchmark datasets except TLDR. For TLDR, the provided judge-assigned scores from older LLMs are used: GPT-4-0314, GPT-3.5-Turbo-0301, and Llama-2-70b-chat-hf.

To mitigate position bias, the order of candidate responses presented to judges was randomized.

D.3 LLM candidates

For consistent comparison across datasets, the set of candidate LLMs shown in Table D.1 was evaluated.

Table D.1: LLM candidates evaluated across all experimental settings

Model Family	Model Name	Version/Date	Experiments
Anthropic	Claude 3.5 Haiku	claude-3-5-haiku-20241022	GPQA, MMLU Pro, Omni-MATH
Anthropic	Claude 3.5 Sonnet	claude-3-5-sonnet-20241022	GPQA, MMLU Pro, Omni-MATH
Anthropic	Claude 3.7 Sonnet	claude-3-7-sonnet-20250219	GPQA, MMLU Pro, Omni-MATH
DeepSeek	DeepSeek V3	deepseek-v3	GPQA
Google	Gemini 1.5 Flash	gemini-1.5-flash-002	GPQA, MMLU Pro, Omni-MATH
Google	Gemini 1.5 Pro	gemini-1.5-pro-002	GPQA, MMLU Pro, Omni-MATH
Google	Gemini 2.0 Flash	gemini-2.0-flash-001	GPQA, MMLU Pro, Omni-MATH
Google	Gemini 2.0 Flash Lite	gemini-2.0-flash-lite-preview-02-05	GPQA, MMLU Pro, Omni-MATH
Meta	Llama 3.1 405B	llama-3.1-405b-instruct-turbo	GPQA, MMLU Pro, Omni-MATH
Meta	Llama 3.1 70B	llama-3.1-70b-instruct-turbo	GPQA, MMLU Pro, Omni-MATH
Meta	Llama 3.1 8B	llama-3.1-8b-instruct-turbo	GPQA, MMLU Pro, Omni-MATH
Meta	Llama 4 Maverick 17B	llama-4-maverick-17b-128e-instruct-fp8	MMLU Pro, Omni-MATH
Meta	Llama 4 Scout 17B	llama-4-scout-17b-16e-instruct	MMLU Pro, Omni-MATH
Mistral AI	Mistral 7B	mistral-7b-instruct-v0.3	GPQA
Mistral AI	Mixtral 8x22B	mixtral-8x22b-instruct-v0.1	GPQA
Mistral AI	Mixtral 8x7B	mixtral-8x7b-instruct-v0.1	GPQA
OpenAI	GPT-4.1	gpt-4.1-2025-04-14	MMLU Pro, Omni-MATH
OpenAI	GPT-4.1 mini	gpt-4.1-mini-2025-04-14	MMLU Pro, Omni-MATH
OpenAI	GPT-4.1 nano	gpt-4.1-nano-2025-04-14	MMLU Pro, Omni-MATH
OpenAI	GPT-4o	gpt-4o-2024-11-20	GPQA, MMLU Pro, Omni-MATH
OpenAI	GPT-4o mini	gpt-4o-mini-2024-07-18	GPQA, MMLU Pro, Omni-MATH
Qwen	Qwen 2.5 72B	qwen2.5-72b-instruct-turbo	GPQA, MMLU Pro, Omni-MATH
Qwen	Qwen 2.5 7B	qwen2.5-7b-instruct-turbo	GPQA, MMLU Pro, Omni-MATH

For the MTBench dataset (Zheng et al., 2023), the candidates in the provided dataset are assessed: GPT-4-0613, Claude-1, Llama-2-13B-Chat, Vicuna-13B, and Alpaca-13B. Similarly, for the TLDR (SummEval) benchmark (Fabbri et al., 2021), the 12 provided language models are assessed.

D.3.1 Comparison Methods

The Bayesian adjudication framework is compared against the following baseline methods:

Simple Averaging: This approach computes the mean score for each candidate across all evaluations and determines rankings based on these averages. It treats each judge's assessment with equal weight and assumes judge scores accurately reflect true performance.

Single Judge Aggregation: This approach collapses distinctions between multiple judges, treating all evaluations as if they came from a single judge. It computes the mean score for each candidate across all judge evaluations, ignoring judge identity.

Simple Averaging with Bootstrap Confidence Intervals: This comparator uses the bootstrap approach for population ranks proposed in Xie et al. (2009) to generate confidence intervals for the simple averaging estimate.

Pairwise Comparison Approach: As a representative pairwise comparison method, an extension of the Bradley-Terry model with ties (Rao and Kupper, 1967) is used, which estimates candidate ability parameters based on win-loss-tie patterns in pairwise evaluations. Confidence intervals are calculated using the bootstrap.

Prediction-Powered Inference (PPI): For benchmarks with ground truth labels, PPI (Angelopoulos et al., 2023) is implemented as an alternative ranking method. PPI uses a small labeled dataset to calibrate predictions from LLM judges on a larger unlabeled dataset, providing statistically valid confidence intervals for candidate rankings. The implementation: (i) randomly partitions questions into labeled and unlabeled sets (using 5% or 10% labeled fractions), (ii) applies the PPI mean estimator using the `ppi_py` library with judge scores converted to a 0-1 scale, and (iii) generates confidence intervals through bootstrap resampling (300 iterations) while maintaining the fixed labeled/unlabeled partition. PPI is applied to GPQA, MMLU Pro, and Omni-MATH benchmarks where ground truth answers are available. Results for different labeled data fractions are presented in Section E.1.

Performance is assessed using Spearman's rank correlation with ground truth rankings when available, and coverage rates of 95% credible/confidence intervals for uncertainty calibration. Together these metrics evaluate both point estimate accuracy and uncertainty calibration across methods.

D.4 Prompts

Below are the prompts used for evaluating candidate answers in each experiment. Where possible, structured generation is used to produce JSON outputs.

D.4.1 Binary Verification Judge Prompt

For the GPQA and MMLU Pro dataset experiments with multiple-choice questions and ground truth answers, the following prompt is used:

```
You are evaluating candidate answers to a multiple-choice question.

- Consistency: How well the candidate's explanation aligns with their final multiple choice selection
    (1-5 scale).
  * 1 = The explanation contradicts the selected answer
  * 2 = Major disconnects between explanation and selected answer
  * 3 = Explanation partially supports the answer with some inconsistencies
  * 4 = Explanation mostly supports the answer with minor inconsistencies
  * 5 = Explanation perfectly aligns with and justifies the selected answer

- Accuracy: Did the candidate select the correct answer choice? (-1 = no, 1 = yes, 0 = unsure)
  * Provide a concise explanation referencing key facts or reasoning that makes the answer correct or
    incorrect

<QUESTION>
[[question]]
</QUESTION>

[[candidates_section]]


Respond with a JSON object containing evaluations for all candidates and ensure that your JSON response
    :
- Uses the exact structure provided below
- Includes only the evaluation without additional preamble or commentary
- Properly escapes any special characters in the reasoning strings

{
  "evaluations" : [
    {
      "model_id": "1",
      "consistency": {
        "reasoning": str,
        "score": int
      },
      "accuracy": {
        "reasoning": str,
```

```
        "score": int
      }
    },
    ...
  ]
}
```

In the actual implementation, the `[[candidates_section]]` placeholder is dynamically populated with candidate answers and explanations using the following format:

```
<CANDIDATE #{i} ANSWER>
{candidate.get(answer_key)}
</CANDIDATE ANSWER>

<CANDIDATE #{i} EXPLANATION>
{rationale}
</CANDIDATE #{i} EXPLANATION>
```

where `{i}` is the candidate number, `{candidate.get(answer_key)}` retrieves the candidate's multiple-choice answer, and `{rationale}` contains their explanation for that answer.

D.4.2 Human Judgement Prompts

MTBench Judge Prompts:
For MTBench, a prompt similar to the original one given to human judges in (Zheng et al., 2023) is used for the single-turn and two-turn cases. As with the binary tasks, the `[[question]]` and `[[candidates_section]]` placeholders are replaced with the prompt and the conversation history using the following format:

```
Please act as an impartial judge and evaluate the quality of the responses provided by AI assistants to
     the user question displayed below. Your evaluation should consider factors such as the helpfulness
    , relevance, accuracy, depth, creativity, and level of detail of their responses. Avoid any
    position biases and ensure that the order in which the responses were presented does not influence
    your decision. Do not allow the length of the responses to influence your evaluation. Do not favor
    certain names of the assistants.Be as objective as possible. Rate the response on a scale of 1 to 5
     (1=Very Bad, 5=Very Good), along with the reasoning.

Initial User Question:
<PROMPT>
[[question]]
</PROMPT>

Assistant Conversation(s):
[[candidates_section]]

{
    "evaluations" : [
    {
        "model_id": "1",
        "overall": {
        "reasoning": str,
        "score": int
        }
    },
    {
        "model_id": "2",
        "overall": {
        "reasoning": str,
        "score": int
        }
    },
    {
        "model_id": "3",
        "overall": {
        "reasoning": str,
        "score": int
```

```
        }
    }
    ]
}
```

The candidate presentation format differs between single-turn and multi-turn evaluations. For single-turn interactions, only the initial response is presented:

```
<CANDIDATE #{i}>
{response1}
</CANDIDATE #{i}>
```

For two-turn interactions, the complete conversation history is presented with delineation between turns:

```
<CANDIDATE #{i}>

<TURN 1>
[User Prompt]
{prompt1}
[Assistant Response]
{response1}
</TURN 1>

<TURN 2>
[User Prompt]
{prompt2}
[Assistant Response]
{response2}
</TURN 2>
</CANDIDATE #{i}>
```

In cases where a candidate fails to respond to the second turn, this absence is explicitly noted:

```
<TURN 2>
[No second turn response provided]
</TURN 2>
```

TLDR (SummEval) Judge Prompts:
For the TLDR (SummEval) dataset, the same evaluation framework as in (Fabbri et al., 2021) is used, assessing news article summarization quality across four criteria: relevance, consistency, fluency, and coherence. Each dimension is evaluated on a 5-point Likert scale with specific definitions to ensure consistent interpretation:

```
Instructions: In this task you will evaluate the quality of summaries written for a news article. You
    will be shown the original article and [[num_candidates]] candidate summaries.

To correctly solve this task, follow these steps:

1. Carefully read the original news article provided below.
2. Read the candidate summaries presented in the <CANDIDATE #i ANSWER> sections.
3. Rate each summary on a scale from 1 (very low) to 5 (very high) based on its relevance, consistency,
     fluency, and coherence. Note that summaries that are very similar on an axis may receive the same
    score.

Definitions:
*   Relevance: The rating measures how well the summary captures the key points of the article.
    Summaries in which all and only the important aspects are contained will receive the highest rating
    .
*   Consistency: The rating measures whether the facts in the summary are consistent with the facts in
    the original article. The summary should stay true to the facts reported and not make up untrue
    information.
*   Fluency: This rating measures the quality of individual sentences: are they well-written and
    grammatically correct?
*   Coherence: This rating measures the quality of all sentences collectively: do they fit together and
     sound natural? Consider the quality of the summary as a whole.

Original news article:
```

```
[[question]]

Candidate Summaries:
[[candidates_section]]

Now provide your scores in the following JSON format. Ensure your response is a single JSON object,
    starting with {{ and ending with }}, and includes evaluations for all [[num_candidates]] candidates
    :

{{
    "evaluations": [
    // Evaluation for Candidate #1
    {{
        "model_id": "1", // Corresponds to Candidate #1
        "relevance": {{
        "reasoning": "Provide your reasoning for the relevance score here.",
        "score": int // Score from 1 to 5
        }},
        "consistency": {{
        "reasoning": "Provide your reasoning for the consistency score here.",
        "score": int // Score from 1 to 5
        }},
        "fluency": {{
        "reasoning": "Provide your reasoning for the fluency score here.",
        "score": int // Score from 1 to 5
        }},
        "coherence": {{
        "reasoning": "Provide your reasoning for the coherence score here.",
        "score": int // Score from 1 to 5
        }}
    }},
    // Add evaluations for Candidate #2, #3, ... up to #[[num_candidates]] following the same structure
    // Example for Candidate #2:
    /*
    {{
        "model_id": "2", // Corresponds to Candidate #2
        "relevance": {{
        "reasoning": "...",
        "score": int
        }},
        "consistency": {{
        "reasoning": "...",
        "score": int
        }},
        "fluency": {{
        "reasoning": "...",
        "score": int
        }},
        "coherence": {{
        "reasoning": "...",
        "score": int
        }}
    }}
    */
    // ... other candidates ...
    ]
}}
```

The `[[question]]` and `[[candidates_section]]` placeholders are filled with the news article and the candidate summaries in the same format as the other datasets.

D.4.3 Semi-verifiable task Judge Prompt

For the Omni-MATH dataset experiments, a two-stage evaluation process is used to assess mathematical reasoning when multiple solution paths may be valid. This measures both standalone solution quality and alignment with

reference solutions.

Stage 1: Evaluation Without Ground Truth:
In the first stage, judge LLMs evaluate candidate solutions based solely on mathematical correctness without access to reference answers, mimicking how human experts might evaluate mathematical work without preconceived notions of the "correct" approach. The prompt uses a 3-point accuracy scale (-1 for incorrect, 0 for partially correct, 1 for correct), with explicit instructions to use the middle category sparingly. The full prompt is:

```
Instructions: Evaluate the quality of candidate answers to mathematical questions. You will be shown
    the original question and [[num_candidates]] candidate answers.

To correctly solve this task, follow these steps:

1. Carefully read the original question to understand what is being asked.
2. Read each candidate answer carefully.
3. Rate each answer according to the criteria below based on general mathematical knowledge and
    reasoning.
4. Provide clear justification for each score with specific references to the candidate's answer.

Rate each answer using the following criteria:

### Accuracy Assessment (1 for correct, 0 for partially correct/borderline, -1 for incorrect)
Based on your mathematical knowledge, how accurate is the candidate answer? Strive to categorize
    answers as either Correct (1) or Incorrect (-1). Reserve the Partially Correct/Borderline (0) score
     for answers that contain significant correct elements but also notable errors or omissions, making
     a definitive Correct/Incorrect judgment difficult, or for answers that are technically correct but
     incomplete in a way that affects the final conclusion.
* 1 (Correct): The answer is mathematically sound, reaches a valid conclusion, and is substantially
    free of errors.
* 0 (Partially Correct / Borderline): The answer contains significant correct elements but also notable
     errors or omissions preventing a clear "Correct" score OR the answer is technically correct but
    misses key steps or context, making it significantly less complete. Use this score sparingly.
* -1 (Incorrect): The answer contains significant mathematical errors or reaches an incorrect
    conclusion.

Question:
[[question]]

Candidates Summaries:
[[candidates_section]]

Respond with a JSON object containing evaluations for all candidates and ensure that your JSON response
    :
- Uses the exact structure provided below
- Includes only the evaluation without additional preamble or commentary
- Properly escapes any special characters in the reasoning strings
- Always output the reasoning before providing a final score

{
  "evaluations" : [
    {
      "model_id": "1",
      "accuracy": {
        "reasoning": str,
        "score": int
      }
    },
    ...
  ]
}
```

Stage 2: Evaluation With Ground Truth Reference:
In the second stage, judge LLMs re-evaluate candidate solutions with access to reference solutions, providing a benchmark for alignment with established approaches while still allowing alternative valid solution paths. The prompt maintains the same 3-point scale but refocuses evaluation on comparison with the reference solution. The

full prompt is:

```
Instructions: Evaluate the quality of candidate answers to mathematical questions. You will be shown
    the original question, the ground truth reference answer, and [[num_candidates]] candidate answers.

To correctly solve this task, follow these steps:

1. Carefully read the original question.
2. Carefully read the ground truth reference answer to understand the correct approach and solution.
3. For each candidate answer:
   - Read the entire response
   - Evaluate it against the ground truth reference answer
   - Score it according to the criteria below
   - Provide clear justification for each score with specific references to both the candidate answer
    and ground truth

Rate each answer using the following criteria relative to the ground truth reference answer:

### Accuracy Assessment (1 for correct, 0 for partially correct/borderline, -1 for incorrect)
Based on the reference answer, how accurate is the candidate answer? Strive to categorize answers as
    either Correct (1) or Incorrect (-1). Reserve the Partially Correct/Borderline (0) score for
    answers that contain significant correct elements but also notable errors or omissions, making a
    definitive Correct/Incorrect judgment difficult, or for answers that are technically correct but
    incomplete in a way that affects the final conclusion compared to the reference.
* 1 (Correct): The answer reaches the same mathematical conclusion as the reference answer (even if
    using a different valid approach) and is substantially free of errors.
* 0 (Partially Correct / Borderline): The answer contains significant correct elements but also notable
     errors or omissions preventing a clear "Correct" score OR the answer is technically correct but
    misses key steps or context provided in the reference, making it significantly less complete. Use
    this score sparingly.
* -1 (Incorrect): The answer reaches a different conclusion from the reference answer or contains
    significant mathematical errors that invalidate the result.

Question:
[[question]]

Ground Truth Reference Answer:
[[ground_truth_answer]]

Candidates Summaries:
[[candidates_section]]

Respond with a JSON object containing evaluations for all candidates and ensure that your JSON response
    :
- Uses the exact structure provided below
- Includes only the evaluation without additional preamble or commentary
- Properly escapes any special characters in the reasoning strings
- Always output the reasoning before providing a final score

{
  "evaluations" : [
    {
      "model_id": "1",
      "accuracy": {
        "reasoning": str,
        "score": int
      }
    },
    ...
  ]
}
```

Combined Analysis:
This two-stage approach enables separate analyses of intrinsic solution quality and reference alignment. The second-stage (reference-based) evaluations serve as pseudo-ground truth when comparing the Bayesian ranking methods against baselines. The first-stage evaluations indicate the judge's standalone mathematical reasoning

ability—how often judges can identify correct solutions without reference answers. The gap between stage-one and stage-two evaluations may also provide a signal about problem difficulty and the capabilities of both candidate and judge models.

In the actual implementation, the `[[question]]`, `[[ground_truth_answer]]`, and `[[candidates_section]]` placeholders are dynamically populated with the mathematical problem statement, reference solution, and candidate solutions, respectively. The candidate solutions are presented in the same format as in the other experimental settings.

D.5 MTBench self-preference

Table D.2 presents the frequency of scores (ranging from 1, low, to 5, high) assigned by the two LLM judges—Claude 3.5 Haiku and GPT-4o mini—to various candidate LLMs based on their responses to two-turn questions from the MTBench dataset. The results suggest self-preference bias in LLM-based evaluations. The Claude 3.5 Haiku judge awarded its predecessor, Claude v1, a high frequency of top scores (48 instances of '5'), surpassing other models like GPT-4 (40 instances of '5'). The GPT-4o mini judge assigned an equal number of perfect '5' scores (50 instances each) to both its own family model, GPT-4, and to Claude v1. While GPT-4o mini gives the same number of top scores to GPT-4 and Claude, the scores from the Claude judge suggest that models receive more favorable evaluations from judges within the same model family, indicating self-preference.

Table D.2: Distribution of scores (1-5) assigned by Claude 3.5 Haiku and GPT-4o mini judges to candidate LLMs on the MTBench two-turn benchmark. Cell values represent the frequency of each score.

	Claude 3.5 Haiku					GPT-4o mini				
Model Name	1	2	3	4	5	1	2	3	4	5
Llama 13B	29	32	11	5	0	43	24	15	0	0
Alpaca 13B	3	33	33	8	3	17	25	29	10	0
Vicuna 13B v1.2	1	7	24	27	19	7	12	19	25	18
Claude v1	0	3	2	21	48	1	6	6	18	50
GPT-3.5 Turbo	0	2	11	38	20	1	7	14	23	37
GPT-4	0	1	6	26	40	0	4	8	20	50

D.6 Score Mapping for Simplex Visualizations

For the probability simplex visualizations of 3+-level Likert scale datasets, the original 5-point scales are mapped to 3-point scales to enable more interpretable simplex representations. The mapping functions $f : \{0, 1, 2, 3, 4, 5\} \mapsto \{1, 2, 3\}$ are defined as follows:

TLDR mapping:

$$f_{\text{TLDR}}(s) = \begin{cases} 1, & \text{if } s \in \{1, 2\} \\ 2, & \text{if } s \in \{0, 3, 4\} \\ 3, & \text{if } s = 5 \end{cases}$$

MTBench mapping:

$$f_{\text{MTBench}}(s) = \begin{cases} 1, & \text{if } s \in \{1, 2\} \\ 2, & \text{if } s \in \{0, 3\} \\ 3, & \text{if } s \in \{4, 5\} \end{cases}$$

The main difference between these mappings is the treatment of score 4. For TLDR, it is grouped with score 3 in the middle category, while for MTBench, it is grouped with score 5 in the top category. These different groupings reflect the empirical distribution patterns observed in each dataset. MTBench evaluations exhibit more separation between high-performing candidates, while TLDR shows finer distinctions between middle performing candidates.

E ADDITIONAL RESULTS

E.1 Prediction-Powered Inference Results

Table E.3 presents ranking results using Prediction-Powered Inference (PPI) across GPQA, MMLU Pro, and Omni-MATH benchmarks with varying amounts of labeled data (5% and 10%). PPI achieves high correlations with true rankings and strong coverage rates. These results confirm that PPI is effective at quantifying uncertainty when calibrated with even small amounts of labeled data, providing reliable confidence intervals while maintaining competitive ranking accuracy. The method's strength is its ability to use limited ground truth to correct for judge bias, making it well suited when some labeled examples are available. In contrast, the Bayesian framework provides robust uncertainty quantification when gold-standard labels are unavailable, addressing the complementary scenario where obtaining any ground truth is impractical.

Table E.3: Performance of PPI ranking method across benchmark datasets with different labeled fractions. Results show Spearman correlation (Corr) and coverage rates (Cov) with 95% confidence intervals.

Labeled Fraction	GPQA		MMLU Pro		Omni-MATH	
	Corr	Cov	Corr	Cov	Corr	Cov
5%	0.773 (0.445, 0.889)	0.889 (0.778, 1.000)	0.902 (0.691, 0.919)	0.947 (0.749, 1.000)	0.789 (0.486, 0.905)	0.895 (0.789, 1.000)
10%	0.875 (0.529, 0.923)	0.944 (0.790, 1.000)	0.922 (0.782, 0.929)	1.000 (0.737, 0.947)	0.737 (0.621, 0.929)	0.895 (0.801, 1.000)

E.2 Posterior Distribution Plots

Figures E.4–E.7 present posterior distributions for candidate rankings across additional benchmarks, complementing the GPQA results in the main text. These visualizations reveal consistent patterns in how different methods quantify uncertainty.

MMLU Pro and Omni-MATH (Figure E.4): Both datasets exhibit similar characteristics to GPQA, with the Bayesian method producing wider credible intervals that capture epistemic uncertainty about judge quality. The increased width is most pronounced for middle-ranked candidates, where judge disagreement tends to be highest. For Omni-MATH, greater overall uncertainty is observed across all methods, consistent with the sensitivity analysis showing this dataset's vulnerability to constancy violations.

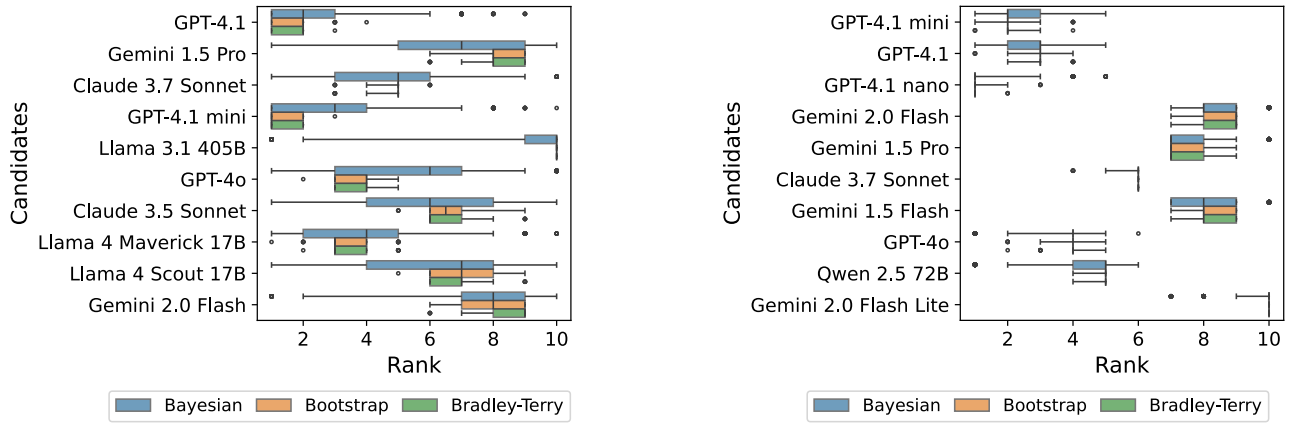

Figure E.4: Posterior distributions for candidate rankings on MMLU Pro (left) and Omni-MATH (right), with candidates ordered by true ranking (best at top).

SummEval (Figure E.7): Across the four evaluation dimensions (coherence, consistency, fluency, and relevance), the Bayesian approach maintains wider intervals while preserving accurate point estimates. The coherence and consistency dimensions show tighter clustering of posterior distributions compared to fluency and relevance, suggesting these aspects may be more reliably evaluated by LLM judges. The top-ranked candidates (M22, M23, M17) show relatively narrow intervals across all methods, indicating strong agreement on the best performers.

MTBench (Figure E.6): The MTBench dataset exhibits tight posterior distributions across all methods, indicating strong judge consensus. Even the Bayesian approach produces relatively narrow credible intervals, suggesting low epistemic uncertainty for this dataset. This aligns with the sensitivity analysis showing MTBench maintains stable rankings under relaxed constancy assumptions, a case where judge-based evaluation is particularly reliable.

A key pattern across all datasets is that while the three methods generally agree on median rankings, they diverge substantially in uncertainty quantification. The Bootstrap and Bradley-Terry methods produce similar narrow confidence intervals that account only for sampling variability. The Bayesian framework's wider intervals reflect both aleatoric and epistemic uncertainty, explaining its superior coverage rates reported in the main text. This difference is most pronounced for candidates with intermediate performance levels, where judge quality uncertainty has the greatest impact on ranking uncertainty.

E.3 Robustness to Self-Preference Bias

While the main experiments demonstrate the framework's ability to handle naturally occurring judge biases (e.g., MTBench self-preference in Table D.2), additional controlled experiments were conducted to systematically evaluate robustness to self-preference bias.

Experimental Design: Using the GPQA dataset, self-preference bias was artificially induced by manipulating judge-assigned scores when judges evaluated candidates from the same model family. Specifically, when Claude judges evaluated Claude candidates or GPT judges evaluated GPT candidates, the assigned score was shifted upward with probability 0.8. This creates a strong but realistic bias pattern similar to that observed in real

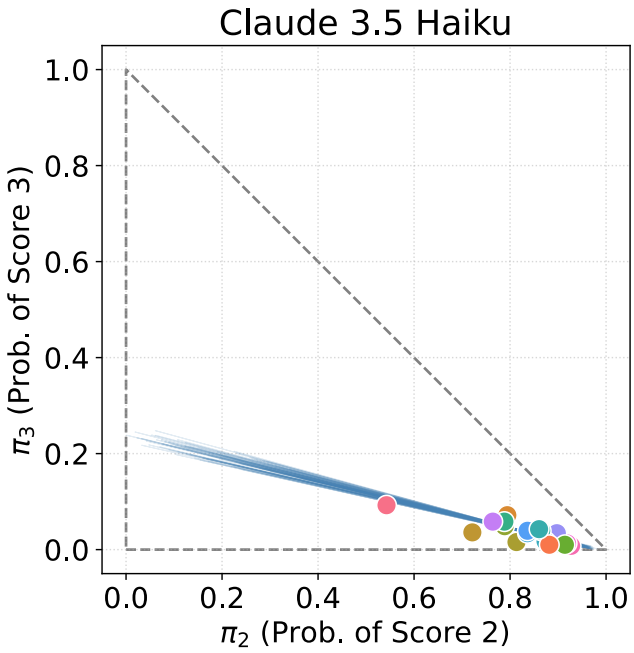

Figure E.5: Candidates visualized on the probability simplex for MMLU Pro, with judge configurations sampled from the posterior (blue line segments). With binary true scores (correct/incorrect) and three assigned score categories (correct, incorrect, abstain), each posterior judge configuration maps to two points on the simplex connected by a line segment. The tight clustering of candidates in the upper region reflects the high overall accuracy on MMLU Pro, while the posterior judge configurations show moderate variability consistent with the sensitivity to constancy violations observed in the main text.

evaluations.

Bias Injection Protocol:

- For binary scores (correct/incorrect), incorrect answers were changed to correct with probability 0.8
- For abstentions, scores were converted to correct with probability 0.8
- Non-self evaluations remained unchanged

This manipulation creates a challenging scenario where traditional averaging methods would systematically overestimate the performance of judge-candidates.

Table E.4: Performance under simulated self-preference bias on GPQA dataset

Method	Correlation	Coverage
Bayesian with self-preference adjustment	**0.811**	**0.852**
Bayesian without adjustment	0.701	0.611
Bootstrap	0.680	0.519
Bradley-Terry	0.673	0.482
Simple Average	0.680	0.056
Single Judge	0.683	0.148

The results demonstrate that the Bayesian framework with self-preference adjustment effectively corrects for the induced bias, achieving correlation and coverage rates comparable to the unbiased setting shown in the main text. Without adjustment, all methods suffer substantial performance degradation, with the Bayesian method's correlation dropping from 0.881 to 0.701.

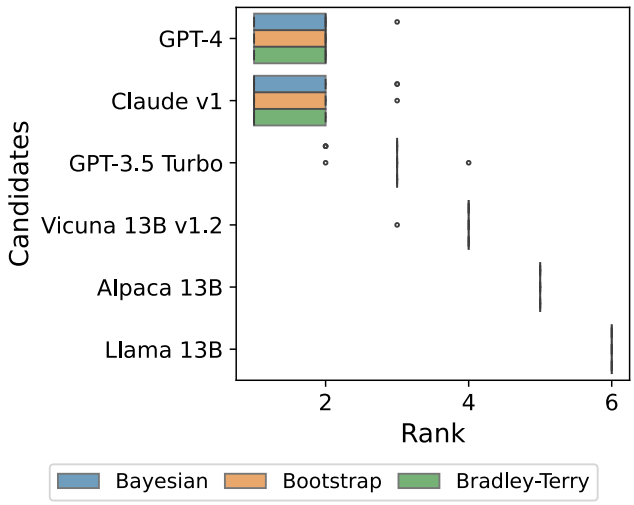

Figure E.6: Posterior distributions for candidate rankings on MTBench, with candidates ordered by true ranking (best at top).

E.4 Prior Specification Comparison

The weight-propagation prior (Section 5.3) encodes structural monotonicity through a directed graph over confusion matrix entries. It is compared against two alternatives: a diagonal-heavy Dirichlet prior that places independent priors on each confusion matrix row with boosted diagonal concentration, and a mixing prior that constructs each row as a convex combination of the preceding row and an innovation term. Table E.5 reports Spearman rank correlation with ground truth and 95% credible interval coverage for each specification across GPQA, MMLU Pro, and Omni-MATH, with 95% bootstrap confidence intervals over 50 resamples.

Table E.5: Spearman correlation and coverage under three prior specifications, with 95% bootstrap confidence intervals. The weight-propagation prior is the only specification with consistently positive correlations and tight confidence intervals across all benchmarks.

Benchmark	Prior	Spearman [95% CI]	Coverage [95% CI]
GPQA	Weight-propagation	0.920 [0.869, 0.946]	0.833 [0.722, 0.889]
GPQA	Diagonal-heavy	−0.558 [−0.932, 0.920]	0.944 [0.013, 0.944]
GPQA	Mixing	**0.921** [−0.936, 0.896]	0.833 [0.056, 0.944]
MMLU Pro	Weight-propagation	**0.940** [0.840, 0.943]	0.895 [0.895, 1.000]
MMLU Pro	Diagonal-heavy	0.809 [−0.878, 0.939]	0.947 [0.749, 1.000]
MMLU Pro	Mixing	−0.886 [−0.906, 0.312]	0.842 [0.064, 0.947]
Omni-MATH	Weight-propagation	**0.811** [0.730, 0.834]	0.737 [0.421, 0.789]
Omni-MATH	Diagonal-heavy	0.251 [−0.769, 0.783]	0.579 [0.486, 0.895]
Omni-MATH	Mixing	−0.758 [−0.817, 0.801]	0.737 [0.404, 0.895]

Both alternative priors exhibit instability: their bootstrap confidence intervals span from strongly negative to strongly positive correlations, indicating that on any given data resample the ranking may be accurate or catastrophically inverted. Each fails through a distinct mechanism.

Confusion matrix collapse (diagonal prior). The diagonal-heavy prior places independent Dirichlet priors on each confusion matrix row with boosted diagonal elements but no inter-row coupling. On GPQA, where judge signal is weak and score marginals are near-balanced, both rows of the confusion matrix collapse toward the marginal distribution of observed scores. All candidates' latent prevalences compress into a narrow range, and the residual variation anti-correlates with ground truth ($\rho = -0.558$). The bootstrap CI [−0.932, 0.920] spans nearly the full range, confirming this instability across resamples. On Omni-MATH, the same mechanism yields a point estimate of only 0.251 with a CI of [−0.769, 0.783].

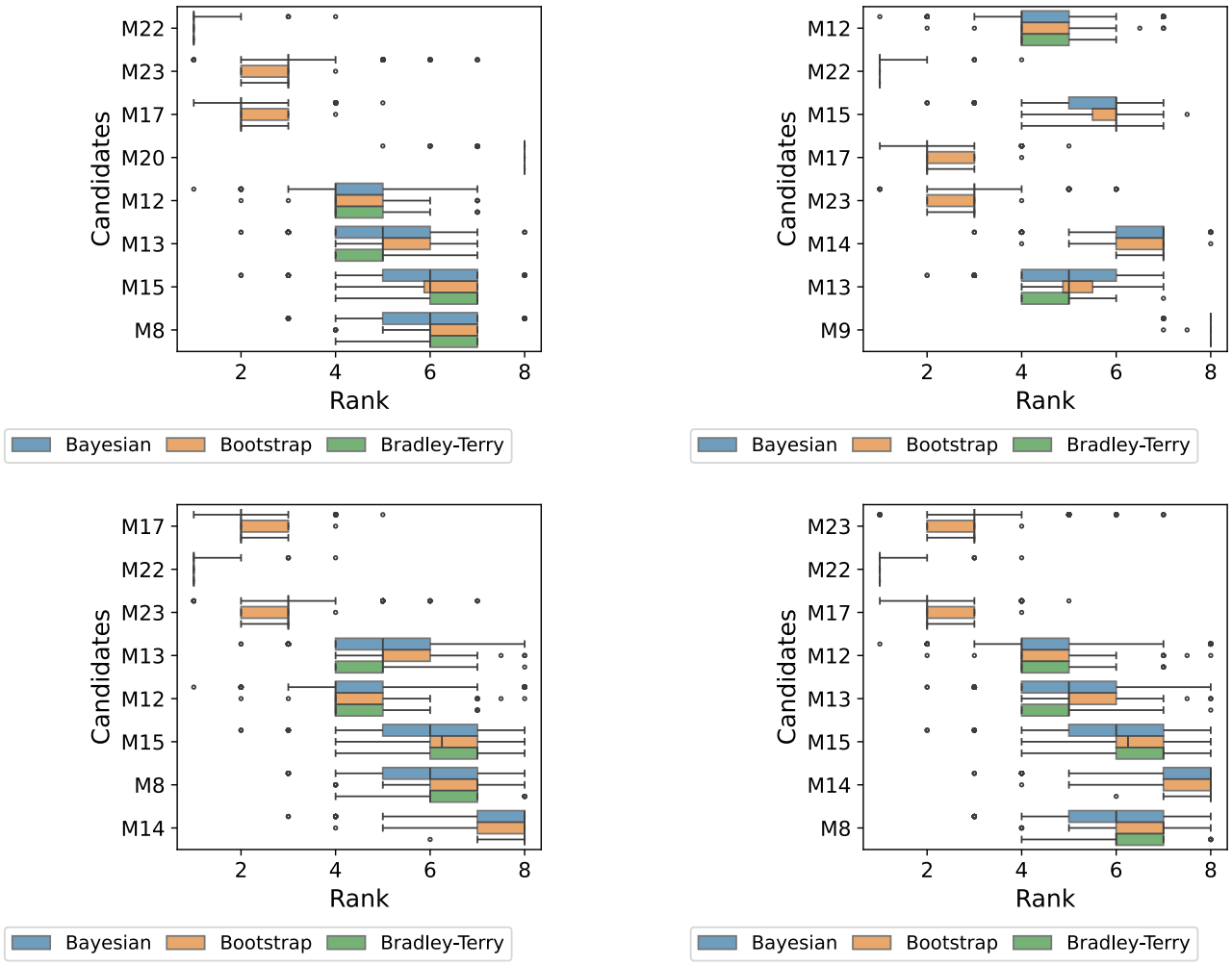

Figure E.7: Posterior distributions for candidate rankings on TLDR/SummEval across four evaluation dimensions: coherence (top left), consistency (top right), fluency (bottom left), and relevance (bottom right). Candidates are ordered by true ranking (best at top).

Label switching (mixing prior). The mixing prior constructs each confusion matrix row as a convex combination of the previous row and an innovation term but lacks monotonicity constraints. On MMLU Pro, the posterior finds a label-switched solution where $P(\text{correct} \mid \text{true} = \text{low}) = 0.839$ exceeds $P(\text{correct} \mid \text{true} = \text{high}) = 0.633$, inverting the labels entirely ($\rho = -0.886$). This is not a convergence failure (only 15 of 4000 transitions are divergent) but a likelihood geometry problem: the label-switched mode is equally valid without structural constraints. The same failure occurs on Omni-MATH ($\rho = -0.758$).

Why weight-propagation succeeds. The weight-propagation prior makes label switching geometrically impossible: probability mass can only shift toward higher assigned scores as the true score increases, so the confusion matrix rows are ordered by construction. This structural monotonicity also prevents collapse by maintaining meaningful separation between rows (L_1 separation > 1.3 vs. 0.25–0.41 for the failing priors). Critically, the weight-propagation prior is the only specification whose bootstrap confidence intervals remain consistently positive across all three benchmarks (Table E.5), confirming its stability under data perturbation.

F PROOFS

This section presents the proofs for the main results. For the identifiability results, recall the following assumptions:

Assumption 1. *Judge $\hat{s}_j$ satisfies "strong constancy" if its confusion matrix is the same across all K candidates: For each m, there is some $\theta_m^{(j)}$ such that $\theta_{m,k}^{(j)} = \theta_m^{(j)}$ for $k = 1, \cdots, K$.*

Assumption 2. *Judge $\hat{s}_j$ satisfies "moderate constancy" if its confusion matrix is the same for all non-self candidates: For each m, there is some $\theta_m^{(j)}$ such that $\theta_{m,k}^{(j)} = \theta_m^{(j)}$ for all $k \neq j$.*

Assumption 3. *The j-th judge's probability of assigning the lowest score when the true score is equal to m decreases with respect to m.*

F.1 Proof for Theorem 1

Proof for Theorem 1(i). By Assumption 1, we have

$$\theta_1 \;=\; \Pr\big(\hat{S}_k = 1 \mid S_k^* = 1\big), \qquad \theta_0 \;=\; \Pr\big(\hat{S}_k = 1 \mid S_k^* = 0\big)$$

for all $k = 1, \cdots, K$. Moreover, by Assumption 3, we have that $\theta_1 > \theta_0$.

For candidate k, let

$$\pi_k \;=\; \Pr\big(S_k^* = 1\big), \qquad \gamma_k \;=\; \Pr\big(\hat{S}_k = 1\big).$$

Then

$$\gamma_k = \; \pi_k\, \theta_1 \;+\; (1 - \pi_k)\, \theta_0.$$

For any set of K candidates with non-equal prevalences of the judge-assigned scores, suppose WLOG that the ordering indices $k_1, \cdots, k_K$ are such that $\gamma_{k_1} > \gamma_{k_2} > \cdots > \gamma_{k_K}$. This implies that

$$\big[\theta_0 + \pi_{k_1}(\theta_1 - \theta_0)\big] \;>\; \big[\theta_0 + \pi_{k_2}(\theta_1 - \theta_0)\big] \;>\; \cdots \;>\; \big[\theta_0 + \pi_{k_K}(\theta_1 - \theta_0)\big]$$

which implies that

$$\pi_{k_1} > \pi_{k_2} > \cdots > \pi_{k_K}.$$

□

Proof for Theorem 1(ii). WLOG, let the candidates who are not also judges (referred to as *core candidates*) have indices $k = 3, 4, \cdots, J$. Let the two LLMs who are both judges and candidates be $k = j \in \{1, 2\}$ (referred to as *judge-candidates*).

Per Assumption 2, we have for each judge $j = 1, 2$ that there exists $\theta_1^{(j)} > \theta_0^{(j)}$ such that

$$\theta_1^{(j)} \;=\; \Pr\big(\hat{S}_k = 1 \mid S_k^* = 1\big), \qquad \theta_0^{(j)} \;=\; \Pr\big(\hat{S}_k = 1 \mid S_k^* = 0\big),$$

for all core candidates k.

Applying our result for Theorem 1(i), we can rank core candidates $k = 3$ and $k = 4$ using their ranking on the line segment from $\theta_1^{(1)}$ to $\theta_0^{(1)}$ (or the line segment from $\theta_1^{(2)}$ to $\theta_0^{(2)}$). Then all core-candidates k can then be jointly ranked (including $k = 3, 4$) by assessing:

$$\frac{\gamma_k^{(1)} - \gamma_k^{(1)}}{\gamma_4^{(1)} - \gamma_3^{(1)}} = \frac{\pi_k - \pi_3}{\pi_4 - \pi_3}.$$

We can rank judge-candidates in a similar way, using their non-self-judged position. Specifically, for candidate $k = 1$, we use its score distribution from judge $j = 2$, i.e. $\gamma_1^{(2)} = \Pr(\hat{S}_1^{(2)} = 1)$, relative to candidates $k = 3$ and $k = 4$ to compute

$$\frac{\gamma_1^{(2)} - \gamma_3^{(2)}}{\gamma_4^{(2)} - \gamma_3^{(2)}} = \frac{\pi_1 - \pi_3}{\pi_4 - \pi_3}.$$

Likewise, for candidate $k = 2$, we use its score distribution from judge $j = 1$, i.e. $\gamma_2^{(1)} = \Pr(\hat{S}_2^{(1)} = 1)$, relative to candidates $k = 3$ and $k = 4$ to compute

$$\frac{\gamma_2^{(1)} - \gamma_3^{(1)}}{\gamma_4^{(1)} - \gamma_3^{(1)}} = \frac{\pi_2 - \pi_3}{\pi_4 - \pi_3}.$$

Thus we have

$$\frac{\gamma_2^{(1)} - \gamma_3^{(1)}}{\gamma_4^{(1)} - \gamma_3^{(1)}} = \frac{\pi_1 - \pi_3}{\pi_2 - \pi_3}.$$

By ranking these shifted and scaled judge-assigned score distributions, we can recover the true ranking between all candidates. □

F.2 Necessary and Sufficient Conditions for 2-Level Systems

While Theorem 1 provides sufficient conditions for ranking identifiability under constancy assumptions, the exact necessary and sufficient conditions for when rankings are preserved in 2-level systems with a single judge can also be characterized.

Lemma 1. *Let $(k_1, k_2, \ldots, k_K)$ be a permutation such that the true scores satisfy $\Pr(S^*_{k_1} = 2) > \Pr(S^*_{k_2} = 2) > \cdots > \Pr(S^*_{k_K} = 2)$. Then the following are equivalent:*

(i) The judge-assigned scores preserve this ordering: $\Pr(\hat{S}^{(j)}_{k_1} = 2) > \Pr(\hat{S}^{(j)}_{k_2} = 2) > \cdots > \Pr(\hat{S}^{(j)}_{k_K} = 2)$

(ii) For all $\ell \in \{1, \ldots, K-1\}$: $\Pr(\hat{S}^{(j)}_{k_\ell} = 2) > \Pr(\hat{S}^{(j)}_{k_{\ell+1}} = 2)$

Proof. The forward direction (i ⇒ ii) is immediate. For (ii ⇒ i), assume $Pr(\hat{S}_{k_\ell} = 2) > Pr(\hat{S}_{k_{\ell+1}} = 2)$ for every $\ell = 1, \ldots, K-1$. Fix any indices $1 \le i < j \le K$. By repeated transitivity,

$$\hat{p}_{k_i} > \hat{p}_{k_{i+1}} > \cdots > \hat{p}_{k_j},$$

hence $\hat{p}_{k_i} > \hat{p}_{k_j}$. Since this holds for all $i < j$, we obtain the strict chain $\hat{p}_{k_1} > \hat{p}_{k_2} > \cdots > \hat{p}_{k_K}$, proving (i). □

The key insight is that only $K-1$ local inequalities between adjacent candidates need to be verified, rather than all $\binom{K}{2}$ pairwise comparisons. For condition (ii) to hold given the true ranking, the following is required:

Theorem 4 (Necessary and Sufficient Conditions)**.** *Consider a 2-level scoring system with a single judge. True rankings are preserved by judge j for all possible candidate configurations if and only if for each adjacent pair $(k_\ell, k_{\ell+1})$ in the true ranking:*

$$\theta^{(1)}_{2,k_\ell} > \theta^{(1)}_{1,k_{\ell+1}} \quad \textit{(cross-term dominance)} \tag{F.8}$$

$$\theta^{(1)}_{1,k_\ell} \ge \theta^{(1)}_{1,k_{\ell+1}}, \ \textit{and if equal, then } \theta^{(1)}_{2,k_\ell} > \theta^{(1)}_{1,k_\ell} \tag{F.9}$$

$$\theta^{(1)}_{2,k_\ell} \ge \theta^{(1)}_{2,k_{\ell+1}}, \ \textit{and if equal, then } \theta^{(1)}_{2,k_{\ell+1}} > \theta^{(1)}_{1,k_{\ell+1}} \tag{F.10}$$

where $\theta^{(1)}_{m,k} = \Pr(\hat{S}^{(1)}_k = 2 | S^*_k = m)$ represents the judge's confusion matrix entries.

Proof. Condition (ii) from Lemma 1 states that $\Pr(S^*_{k_\ell} = 2) > \Pr(S^*_{k_{\ell+1}} = 2)$ implies $\Pr(\hat{S}^{(1)}_{k_\ell} = 2) > \Pr(\hat{S}^{(1)}_{k_{\ell+1}} = 2)$. Using the notation $\pi_{k,m} = \Pr(S^*_k = m)$ and $\theta^{(1)}_{m,k} = \Pr(\hat{S}^{(1)}_k = 2 | S^*_k = m)$, this becomes:

$$\pi_{k_\ell,2} > \pi_{k_{\ell+1},2} \implies \gamma^{(1)}_{k_\ell} > \gamma^{(1)}_{k_{\ell+1}} \tag{F.11}$$

where $\gamma^{(1)}_k = \theta^{(1)}_{1,k}(1 - \pi_{k,2}) + \theta^{(1)}_{2,k}\pi_{k,2}$ is the judge-assigned score probability.

For (F.11) to hold, we need the difference

$$\begin{aligned} g(\pi_{k_\ell,2}, \pi_{k_{\ell+1},2}) &= \gamma^{(1)}_{k_\ell} - \gamma^{(1)}_{k_{\ell+1}} \\ &= \theta^{(1)}_{1,k_\ell}(1 - \pi_{k_\ell,2}) + \theta^{(1)}_{2,k_\ell}\pi_{k_\ell,2} - \theta^{(1)}_{1,k_{\ell+1}}(1 - \pi_{k_{\ell+1},2}) - \theta^{(1)}_{2,k_{\ell+1}}\pi_{k_{\ell+1},2} \\ &= (\theta^{(1)}_{1,k_\ell} - \theta^{(1)}_{1,k_{\ell+1}}) + (\theta^{(1)}_{2,k_\ell} - \theta^{(1)}_{1,k_\ell})\pi_{k_\ell,2} + (\theta^{(1)}_{1,k_{\ell+1}} - \theta^{(1)}_{2,k_{\ell+1}})\pi_{k_{\ell+1},2} \end{aligned} \tag{F.12}$$

to be positive for all $\pi_{k_\ell,2} > \pi_{k_{\ell+1},2}$ with $0 \le \pi_{k_{\ell+1},2} \le \pi_{k_\ell,2} \le 1$.

Since $g(\pi_{k_\ell,2}, \pi_{k_{\ell+1},2})$ is linear in both arguments, it is positive throughout the feasible region if and only if it is non-negative at all extreme points. The feasible region $\{(\pi_{k_\ell,2}, \pi_{k_{\ell+1},2}) : 0 \le \pi_{k_{\ell+1},2} \le \pi_{k_\ell,2} \le 1\}$ has three extreme points:

At $(0,0)$**:** $g(0,0) = \theta^{(1)}_{1,k_\ell} - \theta^{(1)}_{1,k_{\ell+1}} \ge 0$

At $(1,0)$**:** $g(1,0) = \theta^{(1)}_{1,k_\ell} - \theta^{(1)}_{1,k_{\ell+1}} + (\theta^{(1)}_{2,k_\ell} - \theta^{(1)}_{1,k_\ell}) = \theta^{(1)}_{2,k_\ell} - \theta^{(1)}_{1,k_{\ell+1}} > 0$

At $(1,1)$**:** $g(1,1) = \theta^{(1)}_{1,k_\ell} - \theta^{(1)}_{1,k_{\ell+1}} + (\theta^{(1)}_{2,k_\ell} - \theta^{(1)}_{1,k_\ell}) + (\theta^{(1)}_{1,k_{\ell+1}} - \theta^{(1)}_{2,k_{\ell+1}}) = \theta^{(1)}_{2,k_\ell} - \theta^{(1)}_{2,k_{\ell+1}} \ge 0$

Note that $g(1,0)$ must be strictly positive since this corresponds to the interior of the feasible region where $\pi_{k_\ell,2} > \pi_{k_{\ell+1},2}$.

For strict inequality in (F.11) when $\pi_{k_\ell,2} > \pi_{k_{\ell+1},2}$, we also need g to be strictly positive when moving slightly away from the boundary points. This requires:

- If $\theta^{(1)}_{1,k_\ell} = \theta^{(1)}_{1,k_{\ell+1}}$, then $\theta^{(1)}_{2,k_\ell} > \theta^{(1)}_{1,k_\ell}$ to ensure $g(\Delta, 0) > 0$ for small $\Delta > 0$
- If $\theta^{(1)}_{2,k_\ell} = \theta^{(1)}_{2,k_{\ell+1}}$, then $\theta^{(1)}_{2,k_{\ell+1}} > \theta^{(1)}_{1,k_{\ell+1}}$ to ensure $g(1, 1-\Delta) > 0$ for small $\Delta > 0$

These conditions correspond exactly to equations (F.8), (F.9), and (F.10). □

Remark 1. *These necessary and sufficient conditions reveal that without constancy assumptions, ranking preservation requires complex coordination between confusion matrices: higher-ranked candidates must have both larger false-positive rates (FPR) and true-positive rates (TPR) than lower-ranked candidates, with the higher rank's TPR exceeding the lower rank's FPR.*

F.3 Proof for Theorem 2

The proof is given for three levels; the extension to more levels is straightforward.

Proof for Theorem 2. The proof is first given for a single judge. It suffices to show that there exist two candidates whose relative rankings cannot be identified from the judge-assigned score distribution alone.

Consider two candidates in the strict interior of the probability simplex, whose marginal judge-assigned score distributions are denoted γ_1 and γ_2. Let us first consider some judge whose vertices are denoted $\Theta = \begin{pmatrix}\theta_1 & \theta_2 & \theta_3\end{pmatrix}$, whose vertices are also strictly in the interior of the probability simplex and where Θ has full column rank. Then the distribution of the true scores (the barycentric coordinates) for candidate k is given by $\pi_k = \Theta^{-1}\gamma_k$. The true scores of the two candidates are thus equal if

$$\left(\Theta^{-1}(\gamma_1 - \gamma_2)\right)^\top \begin{pmatrix}0\\1\\2\end{pmatrix} = 0. \tag{F.13}$$

Now it is possible that γ_1 and γ_2 were generated by a slightly different judge with triangle corners defined by $\Theta'_h = \Theta + h\Delta$, where $h \in \mathbb{R}$ and Δ is any matrix such that the columns sum to zero. (As long as h is sufficiently small, Θ'_h is a valid set of judge vertices.) If this other judge were the true judge, then the difference of the true scores between the two candidates would be given by

$$\left((\Theta + h\Delta)^{-1}(\gamma_1 - \gamma_2)\right)^\top \begin{pmatrix}0\\1\\2\end{pmatrix}. \tag{F.14}$$

To prove nonidentifiability of the rankings, it thus suffices to show that for any Θ, there exists $\gamma_1, \gamma_2, \Delta$ such that the score difference (F.14) is zero at $h = 0$, i.e. (F.13) holds, and the derivative of the score difference (F.14) is nonzero, i.e.

$$\nabla_h \left((\Theta + h\Delta)^{-1}(\gamma_1 - \gamma_2)\right)^\top \begin{pmatrix}0\\1\\2\end{pmatrix} \propto \left(\Theta^{-1}(\gamma_1 - \gamma_2)\right)^\top (\Theta^{-1}\Delta)^\top \begin{pmatrix}0\\1\\2\end{pmatrix} \neq 0. \tag{F.15}$$

If this were to hold, then there exists some $h > 0$ such that the true score rankings between two candidates with marginal score distributions γ_1 and γ_2 from a judge with vertices $\Theta - h\Delta$ would be the opposite if the judge instead had vertices $\Theta + h\Delta$.

To find such a γ_1, γ_2, and Δ, let $\bar{\pi} = (\frac{1}{3}, \frac{1}{3}, \frac{1}{3})^T$ and $\pi_1 = \bar{\pi} + \frac{\epsilon a}{2}$, $\pi_2 = \bar{\pi} - \frac{\epsilon a}{2}$, where $a = (1, -2, 1)^T$, and $\epsilon > 0$ and small enough such that π_1 and π_2 belong to the probability simplex. Note that $\pi_1^T \mathbf{1} = \pi_2^T \mathbf{1} = \bar{\pi}^T \mathbf{1} = 1$ since $a^T \mathbf{1} = 0$.

Let $\gamma_k = \Theta \pi_k$ for $k = 1, 2$. Then (F.14) $= 0$ at $h = 0$. To prove that (F.15) $\neq 0$ at $h = 0$, let $u = (\Theta^{-1})^T \begin{pmatrix} 0 \\ 1 \\ 2 \end{pmatrix}$ and $\bar{u} = \frac{\mathbf{1}^T u}{3}$. Define

$$\Delta = (u - \bar{u}\mathbf{1})a^\top \in \mathbb{R}^{3 \times 3}.$$

Because $\mathbf{1}^\top (u - \bar{u}\mathbf{1}) a^T = \vec{0}^\top$, we have constructed a Δ such that every column sums to 0. Moreover, because $\Theta^{-1}(\gamma_1 - \gamma_2) = \epsilon\alpha$, (F.15) simplifies to

$$\begin{aligned} \left(\Theta^{-1}(\gamma_1 - \gamma_2)\right)^\top (\Theta^{-1}\Delta)^\top \begin{pmatrix} 0 \\ 1 \\ 2 \end{pmatrix} &= u^T \Delta \epsilon a = u^T (u - \bar{u}\mathbf{1}) a^T a \epsilon \\ &= \sum_{m=1}^{3} (u_m - \bar{u})^2 \|a\|^2 \epsilon \\ &\geq 0. \end{aligned}$$

Now we prove that the inequality is in fact strict. We do this by contradiction. In particular, note that the equity holds if and only if $\vec{u} = (\Theta^{-1})^T \begin{pmatrix} 0 \\ 1 \\ 2 \end{pmatrix} = c\vec{1}$ for some $c \in \mathbb{R}$. Left-multiplying all elements in the equality by $\Theta^\top$, this is equivalent to assuming

$$\Theta^\top \vec{u} = \begin{pmatrix} 0 \\ 1 \\ 2 \end{pmatrix} = c\Theta^\top \vec{1}.$$

However, because each column of Θ is a probability vector, this would imply that $(0, 1, 2) = c\vec{1}$, which would be a contradiction. This implies the score derivative is strictly nonzero.

Note that by adding more judges, the non-identifiability results remain the same. We can still find candidates and judges that satisfy the above conditions.

□

References

Anastasios N Angelopoulos, Stephen Bates, Clara Fannjiang, Michael I Jordan, and Tijana Zrnic. Prediction-powered inference. *Science*, 382(6671):669–674, November 2023.

Alexander R Fabbri, Wojciech Kryściński, Bryan McCann, Caiming Xiong, Richard Socher, and Dragomir Radev. SummEval: Re-evaluating summarization evaluation. *Trans. Assoc. Comput. Linguist.*, 9:391–409, April 2021.

Bofei Gao, Feifan Song, Zhe Yang, Zefan Cai, Yibo Miao, Qingxiu Dong, Lei Li, Chenghao Ma, Liang Chen, Runxin Xu, Zhengyang Tang, Benyou Wang, Daoguang Zan, Shanghaoran Quan, Ge Zhang, Lei Sha, Yichang Zhang, Xuancheng Ren, Tianyu Liu, and Baobao Chang. Omni-MATH: A universal olympiad level mathematic benchmark for large language models. In *The Thirteenth International Conference on Learning Representations*, October 2024.

P V Rao and L L Kupper. Ties in paired-comparison experiments: A generalization of the bradley-terry model. *J. Am. Stat. Assoc.*, 62(317):194, March 1967.

David Rein, Betty Li Hou, Asa Cooper Stickland, Jackson Petty, Richard Yuanzhe Pang, Julien Dirani, Julian Michael, and Samuel R Bowman. GPQA: A graduate-level google-proof Q&A benchmark. *arXiv [cs.AI]*, November 2023.

Stan Development Team. Stan modeling language users guide and reference manual, 2021.

Yubo Wang, Xueguang Ma, Ge Zhang, Yuansheng Ni, Abhranil Chandra, Shiguang Guo, Weiming Ren, Aaran Arulraj, Xuan He, Ziyan Jiang, Tianle Li, Max Ku, Kai Wang, Alex Zhuang, Rongqi Fan, Xiang Yue, and Wenhu Chen. MMLU-pro: A more robust and challenging multi-task language understanding benchmark. *arXiv [cs.CL]*, June 2024.

Minge Xie, Kesar Singh, and Cun-Hui Zhang. Confidence intervals for population ranks in the presence of ties and near ties. *J. Am. Stat. Assoc.*, 104(486):775–788, June 2009.

Lianmin Zheng, Wei-Lin Chiang, Ying Sheng, Siyuan Zhuang, Zhanghao Wu, Yonghao Zhuang, Zi Lin, Zhuohan Li, Dacheng Li, E Xing, Haotong Zhang, Joseph E Gonzalez, and Ion Stoica. Judging LLM-as-a-judge with MT-bench and chatbot arena. *Neural Inf Process Syst*, abs/2306.05685, June 2023.